WEST VIRGINIA UNIVERSITY
COLLEGE OF ENGINEERING, MORGANTOWN, W. VA.

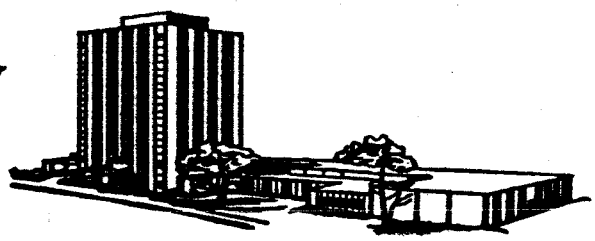

DEPARTMENT OF AERO-SPACE ENGINEERING

AN EXPERIMENTAL STUDY OF VISCOUS-FLOW NOSE-SHAPE EFFECTS ON IMPACT TUBES

BY
Millard L. Howard
Graduate Research Assistant

January 3, 1966

This work was performed under the sponsorship of The National Aeronautics and Space Administration by NASA Grant NsG-533/49-001-001.

Approved: Richard E. Walters
Richard E. Walters
Principal Investigator

ACKNOWLEDGEMENTS

The author wishes to express his appreciation to Richard E. Walters, Instructor in Aerospace Engineering at West Virginia University, for discussions concerning theory and experimentation; to C. A. Murphy for his help in machining part of the equipment; to John Price, Jim Wilson, and Charles Corder for their help in constructing the apparatus and reducing the data; and to his wife and typist, Nancy Lee, for her continued understanding and encouragement.

Appreciation is also expressed to the National Aeronautics and Space Administration for financial support under NASA Grant NsG-533/49-001-001.

TABLE OF CONTENTS

TABLE OF CONTENTS (continued)

LIST OF TABLES

LIST OF FIGURES

LIST OF FIGURES (continued)

LIST OF SYMBOLS

C_p	Pressure Coefficient
g	Acceleration of Gravity
h	Manometer Fluid Height
l	Pitot Tube Height
P	Pressure
V	Velocity

SUBSCRIPTS

$()_a$	Atmospheric Conditions
$()_i$	Stagnation Conditions
$()$	Static Conditions

GREEK SYMBOLS

ρ	Fluid Density
ν	Kinematic Viscosity

ABSTRACT

An experimental investigation was performed using water and three oils of different viscosities along with a series of pitot tubes of different nose shapes to determine the effects of viscosity and nose shape on pitot tube pressure measurements. Data were collected by means of a rotating arm propelling the pitot tubes through stationary fluids in a circular trough. The only appreciable error was considered to be due to the induced motion of the fluid in the trough. No satisfactory means of determining this error was found.

The results were presented in the form of pressure coefficient ($C_p = 2\Delta p/\rho V^2$) as a function of Reynolds number ($Re = Vd/\nu$). (Δp = difference between impact and static pressures, ρ = fluid density, V = free-stream velocity, d = pitot tube diameter, ν = fluid kinematic viscosity.) These results were found to compare favorably with experimental and theoretical results of previous investigations. It was determined that data for similar nose shapes but with different ID/OD (Inside Diameter/Outside Diameter) ratios agree better with Reynolds number based on the OD for square-nosed tubes and with Reynolds number based on ID for hemispherical- and flat-oval-nosed tubes. It was also determined that for the same ID/OD hemispherical-nosed tubes indicate higher pressures than do square-nosed tubes.

INTRODUCTION

The pitot tube is one of the most frequently used measuring devices in the aerodynamics laboratory, and has many applications in fluid flows. The quantity measured, total or stagnation pressure, is useful in determining the energy level and velocity of the fluid. However, several factors can influence the accuracy of the measurements taken. Among these factors are stream turbulence level, tube proximity to the fluid boundary (wall or surface), tube geometry, and fluid viscosity. This study was concerned with the effects of tube geometry and fluid viscosity.

It has been established by previous experiments (7-15)* that at low Reynolds numbers ($Re < 1000$) the viscous forces of the fluid override the inertia forces. This causes the pressure coefficient (C_p) to become increasingly greater than unity with decreasing Reynolds numbers, where

$$Re = \frac{Vd}{\nu}$$

$$C_p = \frac{P_i - P}{\frac{\rho V^2}{2}}$$

It has also been shown that in some cases values of $C_p < 1.0$ are obtained for a range of Reynolds numbers of approximately $20 < Re < 1000$.

---

* Numbers in parentheses refer to references listed in the bibliography.

Although different nose shapes have been investigated, there has been no direct comparison of nose-shape effects coupled with viscous effects. R. G. Folsom (7) has compiled and compared a number of experiments but since all these experiments were performed at different times under different conditions, no reliable conclusions may be drawn. It has also been indicated that orifice size affects the readings.

The purpose of this investigation was to study nose-shape effects and viscous effects simultaneously. By doing this it was hoped that insight could be provided as to what nose shapes are especially influenced by viscosity. Means of correlating data were also investigated, i.e., does data for similarly shaped tubes but with different inside to outside diameter ratios agree with Reynolds number based on inside diameter, outside diameter, or some compromise of the two?

The results of the author were compared with experimental and theoretical data from previous investigations.

LITERATURE SURVEY

As early as 1922, an investigation was made by M. Barker (4) which indicated that at low Reynolds numbers the indicated pressure increases far above that predicted by Bernoulli's equation. Since that time many experimental investigations have been made to find a satisfactory correction factor so that Bernoulli's equation may be used in the regime of low Reynolds numbers. Analytical investigations have also been made for various nose shapes in an attempt to predict the indicated pressure.

Homann (8) and Chambre [from Folsom (7)] made analytical investigations for the pressure at the stagnation point of a sphere. Later experimental work by Homann was in generally good agreement with his theory. Both these analytical investigations were based on thin boundary-layer theory which limits their validity to values of Reynolds number greater than about 10. Some other analytical investigations are by Homann (8) for a cylinder and by Ipsen [from Folsom (7)] for a prolate spheroid and source shape.

Lester (13) investigated the cylindrical pitot tube analytically and found good agreement with experimental results of MacMillan (14), Hurd, Chesky and Shapiro (11), Barker (4), and others. Lester approached the problem by solving the Navier-Stokes equations numerically. According to Lester, the assumptions made should be valid for Reynolds numbers up to about five. Solutions

for higher Reynolds numbers may be obtained but care should be exercised in interpreting the results.

The work of Hurd, Chesky, and Shapiro (11) involved the use of a rotating arm propelling a pitot tube through viscous fluids. The data of this work indicates values of pressure coefficient less than unity for certain values of Reynolds number ($50 < Re < 1000$).

In an attempt to verify the findings of Hurd, et al., MacMillan (14) performed tests on blunt-nosed pitot tubes but no values of $C_p < 1.0$. MacMillan thus claimed the results of Hurd, et al. to be in error. However, the ID/OD* ratio used by MacMillan was 0.6 as compared with 0.74 used by Hurd, et al. Also, the technique used by MacMillan was to measure the flow through a pipe. In a later work by MacMillan (15) using the same technique, he measured airflow using flattened pitot tubes. The data of this later investigation indicates values of $C_p < 1.0$ for Reynolds numbers of $20 < Re < 1000$.

Other tests have shown similar values of $C_p < 1.0$ for supersonic and hypersonic flow. Tests in supersonic boundary layers and hypersonic flow have shown a definite effect of nose shape on the pressures recorded by pitot tubes at low Reynolds numbers. The data of Sherman (18) and of Bailey and Boylan (3) indicate that thin lipped tubes record lower values of pressure than do cylindrical tubes or tubes with rounded noses. Data of Bailey and Boylan also indicate that orifice size also has a bearing on the measured

---

* Inside Diameter/Outside Diameter

impact pressure. These data indicate that as orifice size decreases for a given outside diameter, so does the measured impact pressure.

TEST APPARATUS

The test apparatus, patterned after reference 11, consisted basically of a torus-shaped trough, in which the fluid remained at rest, while the pitot tubes were driven through the fluid (Figures 3, 4, 5). The pressure differences were recorded on a vertical manometer at the center of rotation.

TROUGH

The trough was constructed of galvanized sheet metal and was lined with polyethalene plastic to prevent leakage (see Figure 4). The diameter of the torus at the trough centerline was ten feet and the trough cross-section was twelve inches wide by fourteen inches deep. The fluid line was two inches below the top, making the total fluid volume approximately 31.41 cubic feet.

The base was constructed of two-by-fours and plywood to support the trough and its contents. The base stood about fourteen inches high so that the top of the trough was approximately twenty-eight inches above the floor. Vertical supports were made to extend to the top of the trough to support the sides; however, it was necessary to use additional horizontal supports of galvanized steel on the inner-most side to prevent buckling.

PITOT TUBES

The pitot tubes (Figures 6, 7) were made from copper tubing with common outside diameters of 0.078 inches. The inside diameters

used were 0.020, 0.028, and 0.046 inches. The combinations used are given in the following table.

TABLE I

Pitot Tube Descriptions

Nose Shape	Outside Diameter	Inside Diameter	Other
Square	0.078 inches	0.046 inches	
Square	0.078	0.028	
Square	0.078	0.020	
Tapered	0.078	0.046	5° taper
Tapered	0.078	0.046	10° taper
Internal Chamfer	0.078	0.046	0.250 Chamfer
Internal Chamfer	0.078	0.046	0.063 Chamfer
Hemispherical	0.078	0.046	0.039 in. nose radius
Hemispherical	0.078	0.028	0.039 in. nose radius
Hemispherical	0.078	0.020	0.039 in. nose radius
Flat Oval			0.028 in. major axis 0.016 in. minor axis
Flat Oval			0.059 in. major axis 0.024 in. minor axis

All the tubes were made in the Department of Aerospace Engineering machine shop at West Virginia University. Each tube was threaded on the butt end to connect with the propelling mechanism.

PROPELLING MECHANISM

The pitot tubes were propelled through the fluid by means of a rotating arm (Figure 4) driven by an electric motor through a worm-gear speed reducer. A vertical pipe was fastened to and rotated with the speed reducer output shaft. The arm was fastened to

this vertical pipe and it in turn rotated with the shaft.

The arm extended outward to the centerline of the trough where a streamlined strut extended vertically downward into the fluid. The strut consisted of a brass tube running inside an airfoil shaped fairing. A brass connector threaded to receive the pitot tubes was fastened to the bottom of the strut. This was done to facilitate rapid and easy tube changes.

The speed reducer was run by a belt drive from the electric motor with a pulley ratio of approximately 3.4 to one. The gear ratio in the speed reducer was thirty to one making a total speed reduction of approximately 105 to 1 from the motor to the propelling arm.

The motor was rated as 3/4 horsepower with a maximum speed of 1750 revolutions per minute. It was equipped with an attachment for General Radio Variac which permitted the speed of the motor to be varied over a total possible range of speeds of zero to 1750 revolutions per minute.

The velocity of the rotating arm was determined by timing a specified number of revolutions (usually 10 revolutions) with a stop watch for given settings on the variac.

PRESSURE MEASUREMENTS

Changes in pressure were recorded on a manometer tube housed in the vertical pipe above the speed reducer (Figure 4). The manometer rotated with the vertical pipe and portions of the pipe were cut out so that readings could be taken. The manometer was connected

to the strut tube with plastic tubing which allowed the pressures to travel from the pitot tube through the strut tube and plastic lead-in and to be recorded on the manometer. The manometer fluid was the same as the test fluid. A Wild model T2 theodolite was used to read the changes in manometer fluid height.

DAMPING SCREENS

Removable damping screens (Figure 4) were installed in the trough to minimize the fluid velocity induced by the rotating arm. The screens were made of galvanized fly screening attached to u-shaped flat strap about 3/8 inches wide. Sections which were large compared to the pitot tube diameters, were cut out of the screens to allow the passage of the pitot tubes.

TEST PROCEDURE

PRELIMINARY TESTS

Preliminary tests were run with water to eliminate leaks in the system, to eliminate minor structural problems of the apparatus, and to attempt to determine the induced fluid velocity.

Both the leaks in the system and the structural problems were eliminated from the system. However, no satisfactory means of determining the induced velocity was found.

DATA COLLECTION

Data were collected for water and three oils with viscosities of 15.7×10^{-5}, 56.7×10^{-5}, and 356×10^{-5} ft.^{2}/sec. The viscosity of each oil was determined by taking Saybolt viscometer readings after the oil had been put in the trough. This was done to insure against thickening of the thinner oil by any of the thick oil which may have remained in the trough. It was determined from the viscometer readings that the small temperature fluctuations ($\pm 3^{\circ}$) did not significantly change the viscosities of the fluids.

Data were collected for all the pitot tubes in a particular fluid before the fluid was changed. Each tube was run at a number of different velocities over an approximate range of 0.4 fps to 13 fps to cover the widest possible range of Reynolds numbers. Speed readings were taken for each run and the pitot tube was allowed to run until the manometer fluid reached a constant height.

Three successive readings were taken for each run and the average of these readings was used as the datum. This was done to reduce the error in reading. The same procedure was carried out in determining the pitot tube velocity.

DATA REDUCTION

According to Bernoulli's equation for incompressible flow with no viscous forces present

$$P_i + \frac{\rho V_i^2}{2} = P + \frac{\rho V^2}{2}$$

where Pi is the impact pressure and V_i the impact velocity. At the stagnation point the impact velocity is zero so the equation reduces to

$$P_i = P + \frac{\rho V^2}{2}$$

By subtracting P from both sides and dividing through by $\frac{\rho V^2}{2}$ we obtain

$$\frac{P_i - P}{\frac{\rho V^2}{2}} = 1$$

where the pressure coefficient, C_p, is defined as

$$\frac{P_i - P}{\frac{\rho V^2}{2}} = C_p$$

Bernoulli's equation then says that

$$C_p = 1$$

for incompressible flow with no viscous forces.

At very low Reynolds numbers, viscous forces can not be ignored so that Bernoulli's equation no longer holds. In the case of a rotating arm experiment such as this one an expression for the pressure coefficient may be derived in the following manner.

The impact pressure may be expressed by

$$P_i = P_a + \rho g (l + h) + \frac{\rho r^2 \omega^2}{2}$$

where l is the depth of the pitot tube in the fluid, h is the height of the manometer and $\frac{\rho r^2 \omega^2}{2}$ is the dynamic pressure increase due to the rotation of the arm. The static pressure at infinity is expressed by

$$P = P_a + \rho g l .$$

Since $r\omega$ is the tangential velocity of the pitot tube, V^2 may be substituted for $r^2\omega^2$. Then the pressure coefficient becomes

$$C_p = \frac{\rho g h + \frac{\rho V^2}{2}}{\frac{\rho V^2}{2}}$$

$$C_p = 1 + \frac{2gh}{V^2} .$$

Since the height of the manometer fluid was read with a theodolite, which indicates only angles, the angles had to be converted to a linear measurement. This was acheived in the following manner.

The distance from the theodolite to the manometer was determined by reading the angle between the horizontal and a point nine inches vertically downward from the horizontal (Figure 1). The vertical distance was determined by suspending a scale beside the manometer. The distance x can be expressed as

$$x = \frac{y}{\tan \theta}$$

To determine x, y was set at nine inches on the ruler.

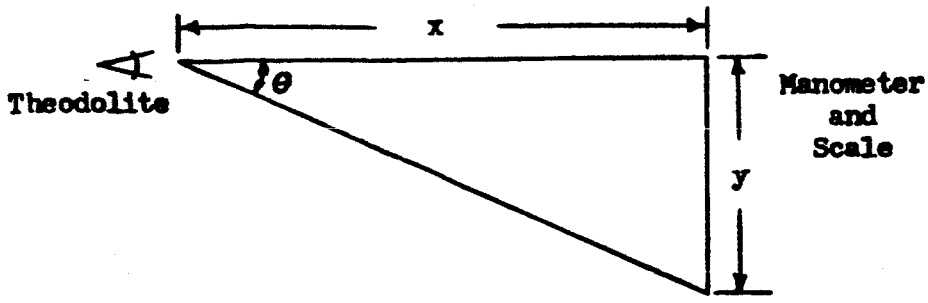

DETERMINATION OF MANOMETER READING CONSTANT

Figure 1

The angle read on the theodolite was

$$\theta = 5°23.95'$$

so

$$x = \frac{9}{\tan(5°23.95')}$$

$$x = 95.228''$$

When taking manometer readings, y becomes the unknown so

$$y = x \tan\theta.$$

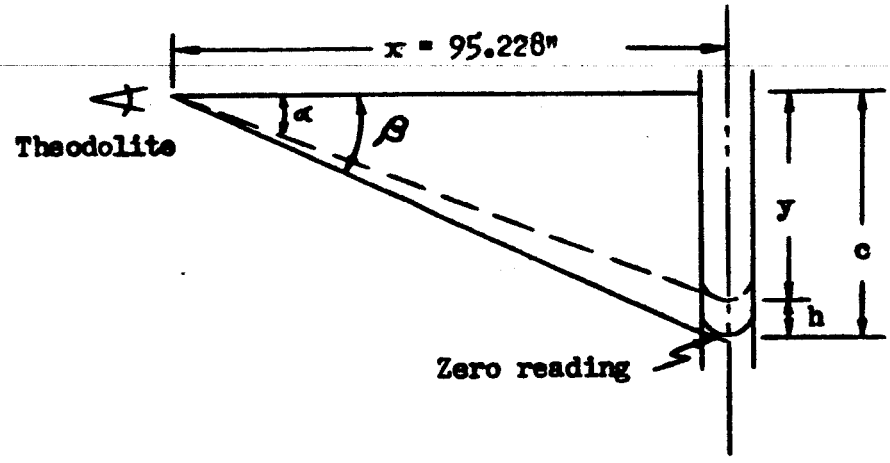

DETERMINATION OF MANOMETER FLUID HEIGHT

Figure 2

From Figure 2 $\theta = \beta$ for the zero reading ($V = 0$). Then

$$y = c = 95.228 \tan\beta .$$

When the pitot tubes are being run, $\theta = \alpha$

and $$y = 95.228 \tan\alpha = c - h$$

or $$h = c - 95.228 \tan\alpha$$

If the fluid were without viscosity the dynamic pressure rise should be exactly canceled by the centrifugal pressure drop and the displacement h should be zero. This would give a C_p equal to unity.

SOURCES OF ERROR

The estimated maximum errors in raw data are as follows:

Tube alignment	2°
Radius of pitot tube travel	1/16"
Time readings	0.010 minutes
Manometer readings	0.15 inches
Saybolt Universal Seconds	0.5 seconds
Temperature	0.5° F

The largest overall source of error is considered to be the induced rotation of the fluid in the tank. No satisfactory method of determing the induced fluid velocity was devised; therefore, the error due to fluid motion was not determinable. An average error was estimated on the basis of the average deviation from $C_p = 1$ at the high Reynolds numbers. This error was estimated at 2%.

Except at the very low speeds, the overlap of data is very good for a given Reynolds number at different speeds. This indicates that pitot tube bending and free surface effects were negligible. If these effects were not negligible, the curves would not fair in so well.

The accuracy of the data points at the two lowest speeds is questionable. From the data for water and the two oils of intermediate viscosities the indicated values of pressure at the two lowest speeds are low compared to values at corresponding Reynolds numbers at higher speeds. This is believed to have been caused by one of three things: frictional drag in the lead-in tube due to

viscous action along the tube walls, centrifugal forces over-riding the impact pressure, or both. If the low data were due to drag in the lead-in tube, the effect should be more pronounced for the more viscous fluids. However, if they were due to centrifugal forces overriding viscous pressure forces, the effect would be more pronounced for the less viscous fluids where fewer particles strike the stagnation point. Since the error is much greater for the more viscous fluids, it is evident that the viscous drag in the lead-in tube is a prominent factor in the pressure readings at the very low speeds.

In light of the foregoing discussion, it is not feasible to estimate the accuracy of the data at the two lowest Reynolds numbers since these data were taken at very low speeds. These values of pressure coefficient are considered to be quite low - possibly 50% or more.

The damping screens introduced a possible error in the pressure field about the pitot tubes. However, the screens were at least ten diameters from the tubes so the error is considered to be negligible.

Tube alignment is not considered to be a source of appreciable error since the deviation was not more than $\pm$ 2°. It has been shown that misalignment does not affect the dynamic pressure reading up to 10° (9, 17). Therefore, error due to pitot tube misalignment is considered negligible.

RESULTS

The data of the present tests are presented in Figures 8 - 18 as pressure coefficient, C_p, versus Reynolds number, Re. In Figures 8, 10, 12, 13, 14 Reynolds number is based on the pitot tube outside diameter, and in Figures 9, 11, 15 Reynolds number is based on inside diameter.

In Figures 8 - 15 the data points with tails attached are considered in error. These data were taken at very low speeds (0.45 - 1.80 fps) in the less viscous fluid in the given range. Comparing these data with data at corresponding Reynolds numbers at higher speeds indicates that these data are in error by 0 - 10% between water and light oil, 3 - 25% between light oil and medium oil, and 13 - 32% between medium oil and heavy oil. The relative accuracy of the data at the lowest Reynolds numbers in the heavy oil is discussed in the section "Sources of Error."

Figures 16, 17, 18 compare the data for different nose shapes but with the same ID/OD ratio. The data in these Figures and in Figures 19 - 23 are presented as smooth curves. All data points have been omitted for purposes of clarity.

Comparisons of the present results with previous experimental results and theoretical results (where available) are made in Figures 19 - 23.

FINDINGS

The results of the author generally agree well with the previous experimental results and with theory. The comparison of results for square-nosed tubes (Figure 19) is good except for the results of MacMillan (14). The reason for this discrepancy is not known. No dip in C_p was observed as indicated by Hurd, et al. (10). Making the 2% correction in C_p as suggested previously would cause the present data to lie along the $C_p = 1$ curve for $Re \geq 80$ based on external radius. Present data is slightly lower than data of Hurd, et al. at low Reynolds numbers.

Agreement between present data and data of Sherman (18) for hemispherical-nosed tubes (Figure 20) is not too good. However, it should be noted that with the Reynolds number based on internal diameter, the agreement with Homann's (8) and Chambre's [from Folsom (7)] theory is quite good. The maximum deviation is approximately 11%.

For the tubes with internal chamfer, agreement is quite good with the data of Sherman (18). It should be noted from Figure 22 that as the chamfer value increases, the measured pressure decreases.

Comparing Figures 8 and 9, data for square-nosed pitot tubes with different ID/OD ratios correlate better with Reynolds number based on the external diameter. Comparing Figures 10 and 11 and Figures 14 and 15, the opposite is true. For hemispherical-nosed and flat-oval-nosed tubes better data correlation is obtained with

Reynolds number based on the internal dimension. Taper-nosed and internal-chamfer-nosed tubes were not tested for Reynolds number characteristic dimension for optimum data correlation.

Figures 16, 17, and 18 indicate that the values of C_p indicated by hemispherical-nosed pitot tubes are generally higher than those values indicated by square-nosed pitot tubes. This fact was previously deduced by MacMillan (14).

No attempts were made to predict the behavior at Reynolds numbers lower than those investigated for two reasons: (1) each tube would require a separate prediction; (2) the accuracy of the data at the two lowest Reynolds numbers investigated is in doubt.

SUGGESTIONS FOR FUTURE WORK

It is suggested that an investigation similar to the author's be performed using heavier oils than used by the author. This would facilitate the acquisition of data at very low Reynolds numbers ($Re < 1$) at high speeds. Such data would eliminate the possible error introduced into the present data by very low speeds.

It is also suggested that similar investigations be performed for pitot tubes at various degrees of yaw. Such an investigation could eliminate another possible source of error.

An effective means of determining the induced motion of the fluid in the tank should be devised. Such knowledge would eliminate the largest source of error introduced into the system.

Internal-chamfer-nosed tubes and flat-oval nosed tubes should be investigated in more detail. Different ID/OD ratios, chamfer values and minor axis/major axis ratios should be investigated to support the trends indicated in Figures 22 and 23.

Taper-nosed and internal-chamfer-nosed tubes should be investigated for optimum data correlation..

Another means of eliminating the induced fluid motion problem would be to use a long straight tank and make runs in one direction. This would necessitate the use of better instrumentation to permit taking measurements quickly.

APPENDIXES

APPENDIX A

TEST APPARATUS

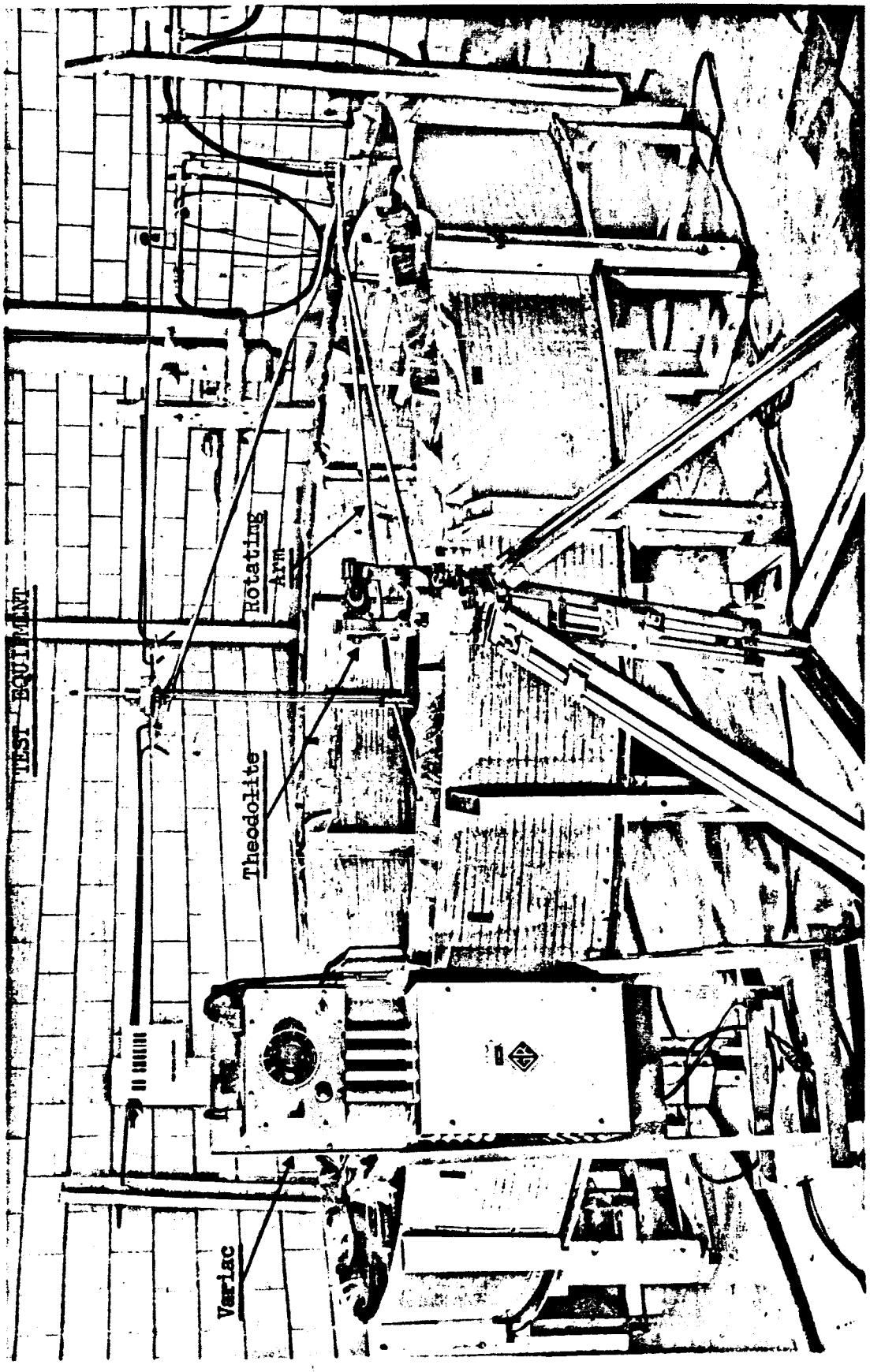

Figure 3

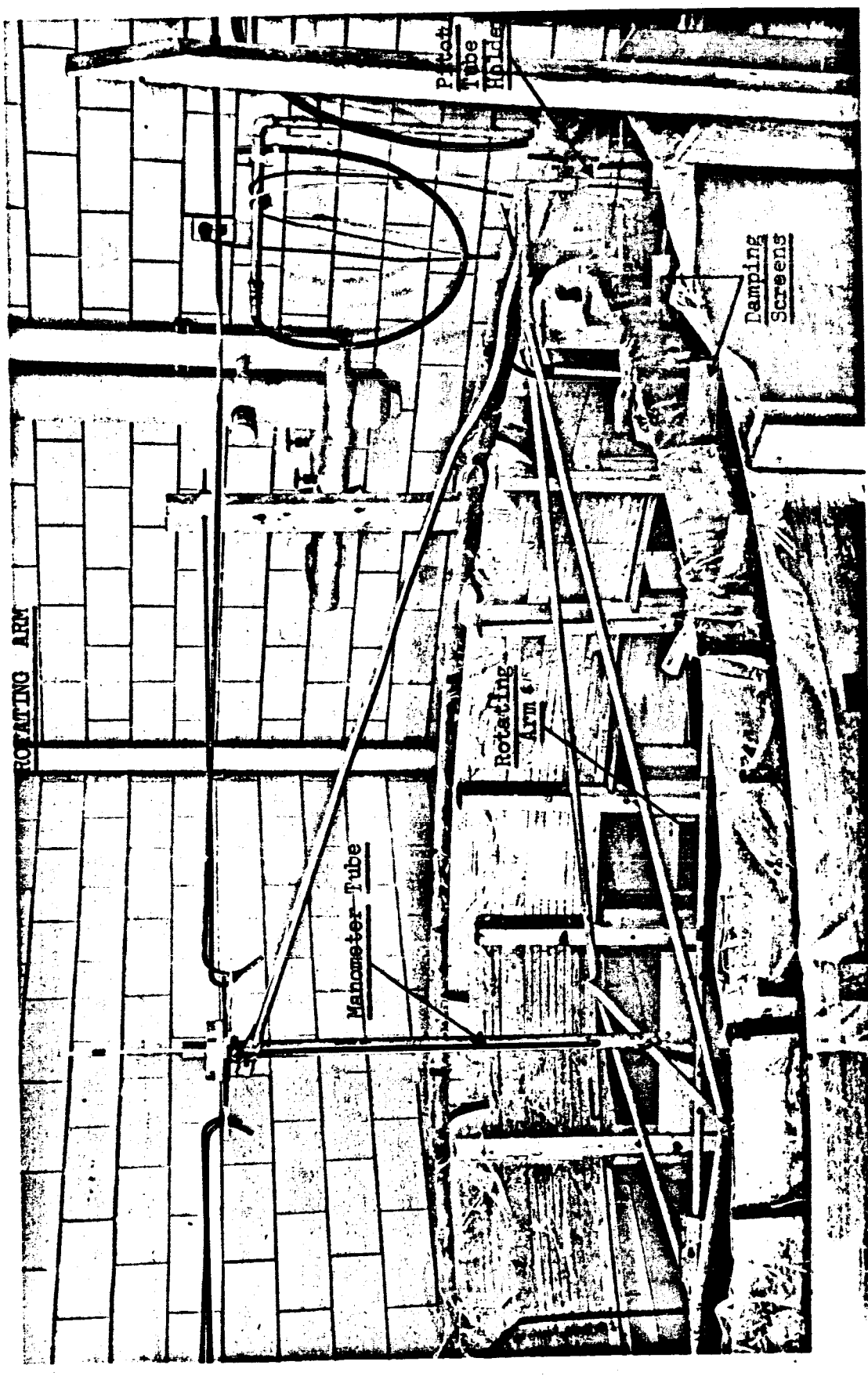
ROTATING ARM
Manometer Tube
Rotating Arm
Pitot Tube Holder
Damping Screens

Figure 4

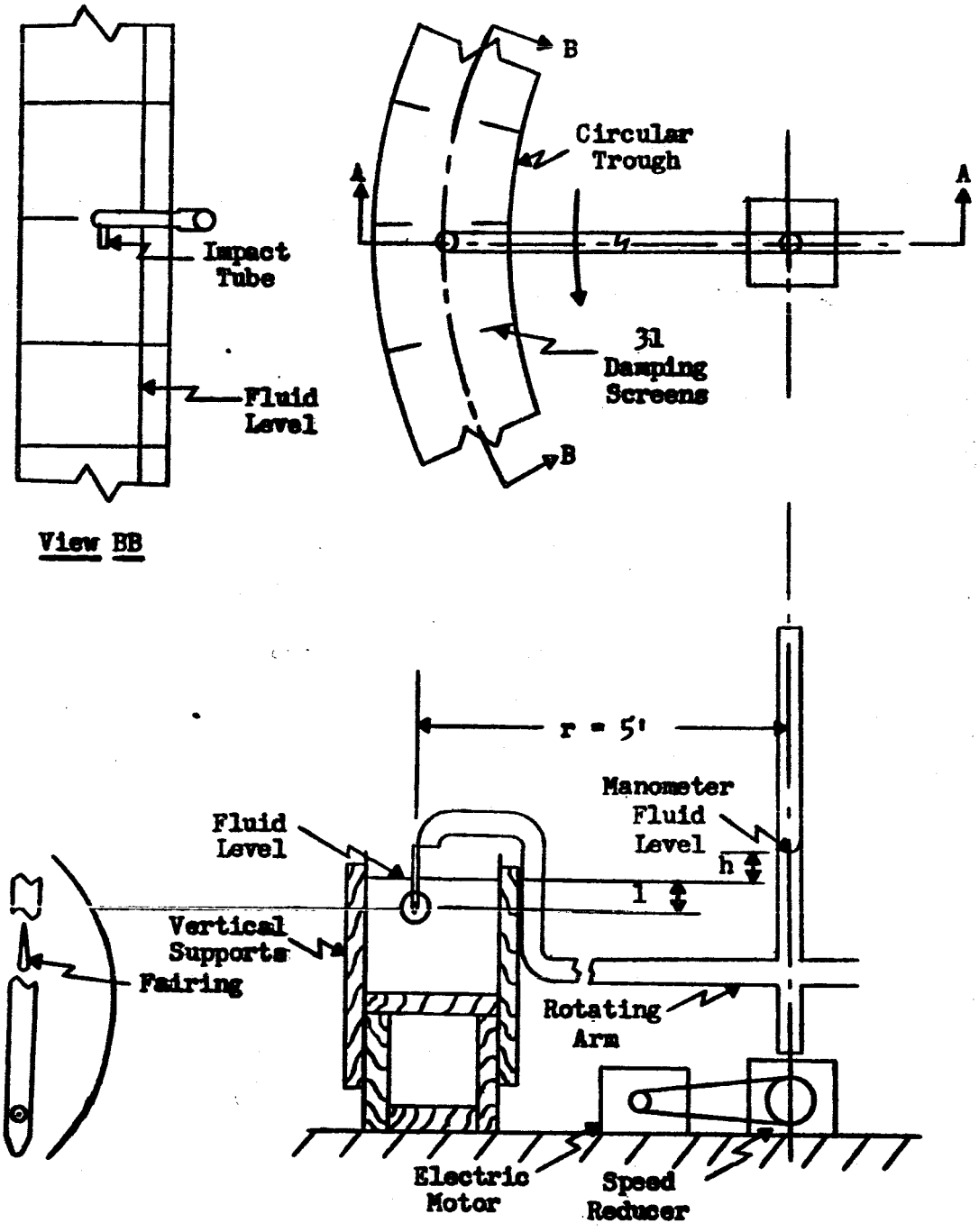

SCHEMATIC OF TEST EQUIPMENT
(Not To Scale)

Figure 5

PITOT TUBES

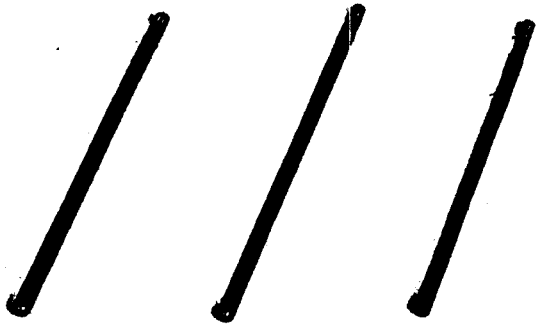

Hemispherical Nose

Square Nose

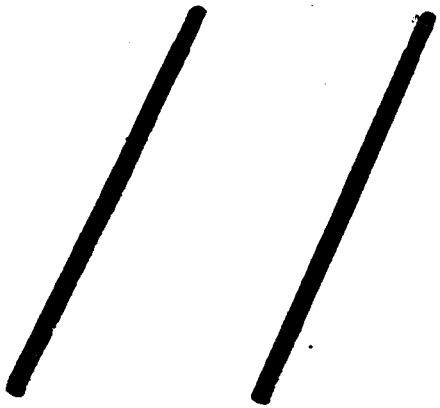

Internal-Chamfer Nose

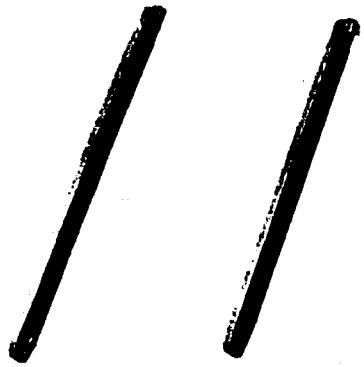

Taper Nose

Flat-Oval Nose

Figure 6

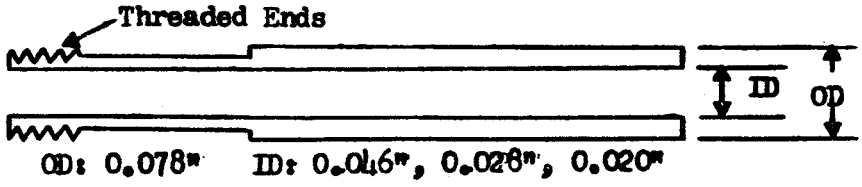

OD: 0.078" ID: 0.046", 0.028", 0.020"

Square Nose

OD: 0.078" ID: 0.046", 0.028", 0.020"
Nose Radius: 0.039"

Hemispherical Nose

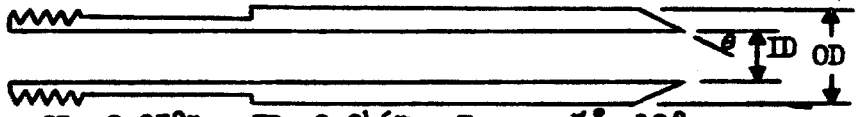

OD: 0.078" ID: 0.046" Taper: 5°, 10°

Tapered Nose

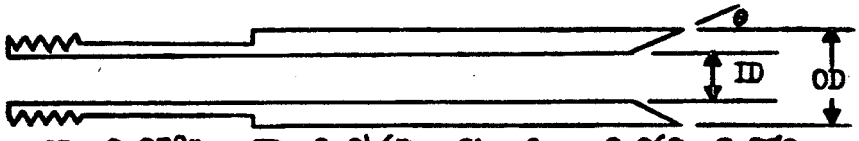

OD: 0.078" ID: 0.046" Chamfer: 0.063, 0.250
Chamfer = tan θ

Internal-Chamfer Nose

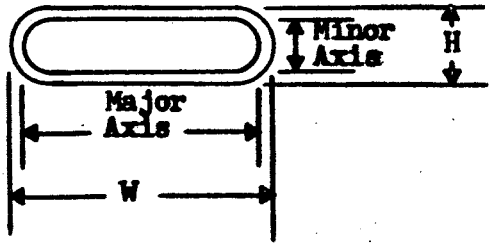

Major Axis: 0.059" 0.028" Minor Axis: 0.024" 0.016"

Flat-Oval Nose

PITOT TUBE NOSE SHAPES
(Not To Scale)

Figure 7

APPENDIX B

EXPERIMENTAL RESULTS

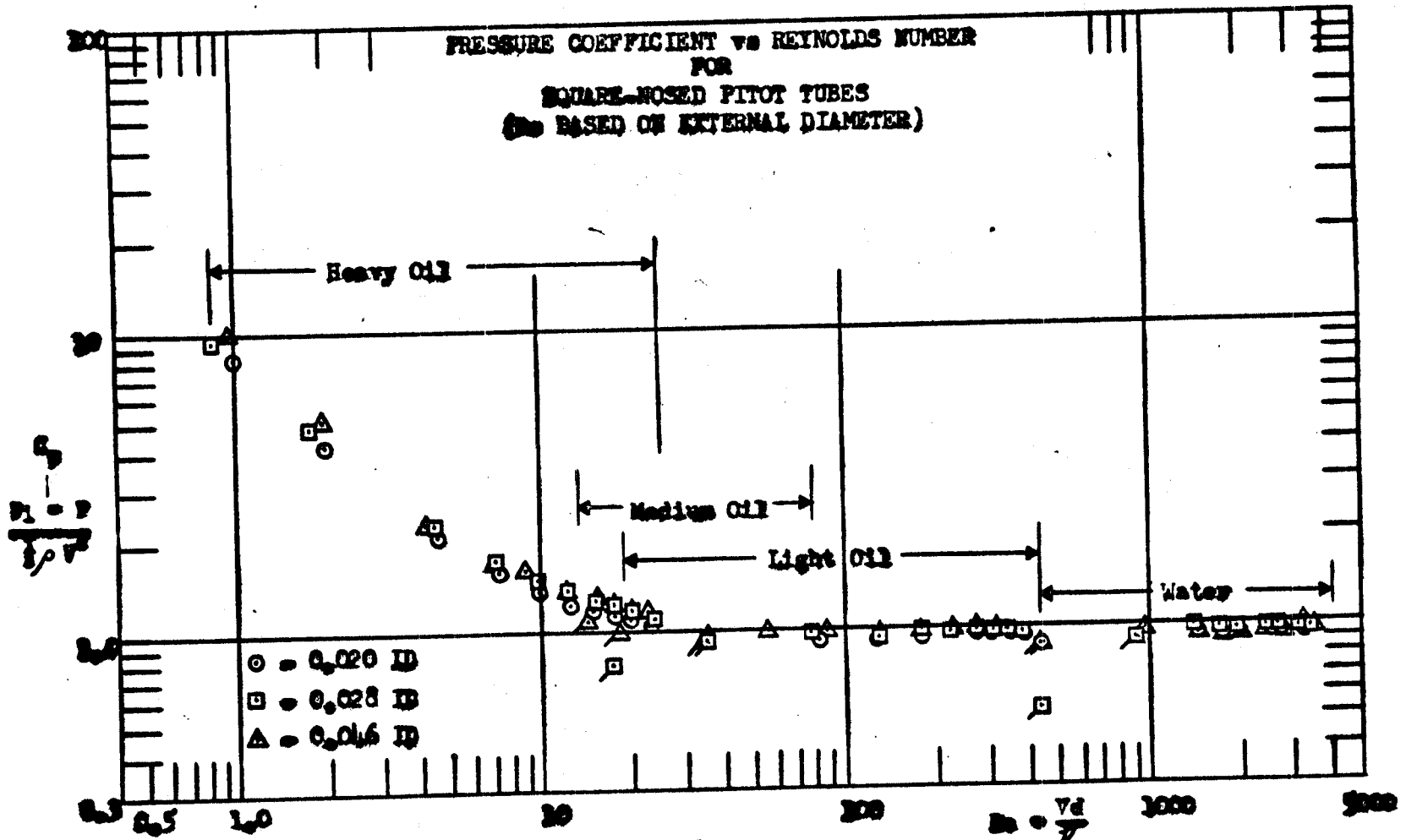
PRESSURE COEFFICIENT vs REYNOLDS NUMBER
FOR
SQUARE-NOSED PITOT TUBES
(Re BASED ON EXTERNAL DIAMETER)
Heavy Oil
Medium Oil
Light Oil
Water
⊙ = 0.020 ID
□ = 0.028 ID
△ = 0.046 ID
0.5
1.0
10
100
1000
Re = Vd/ν

Figure 8

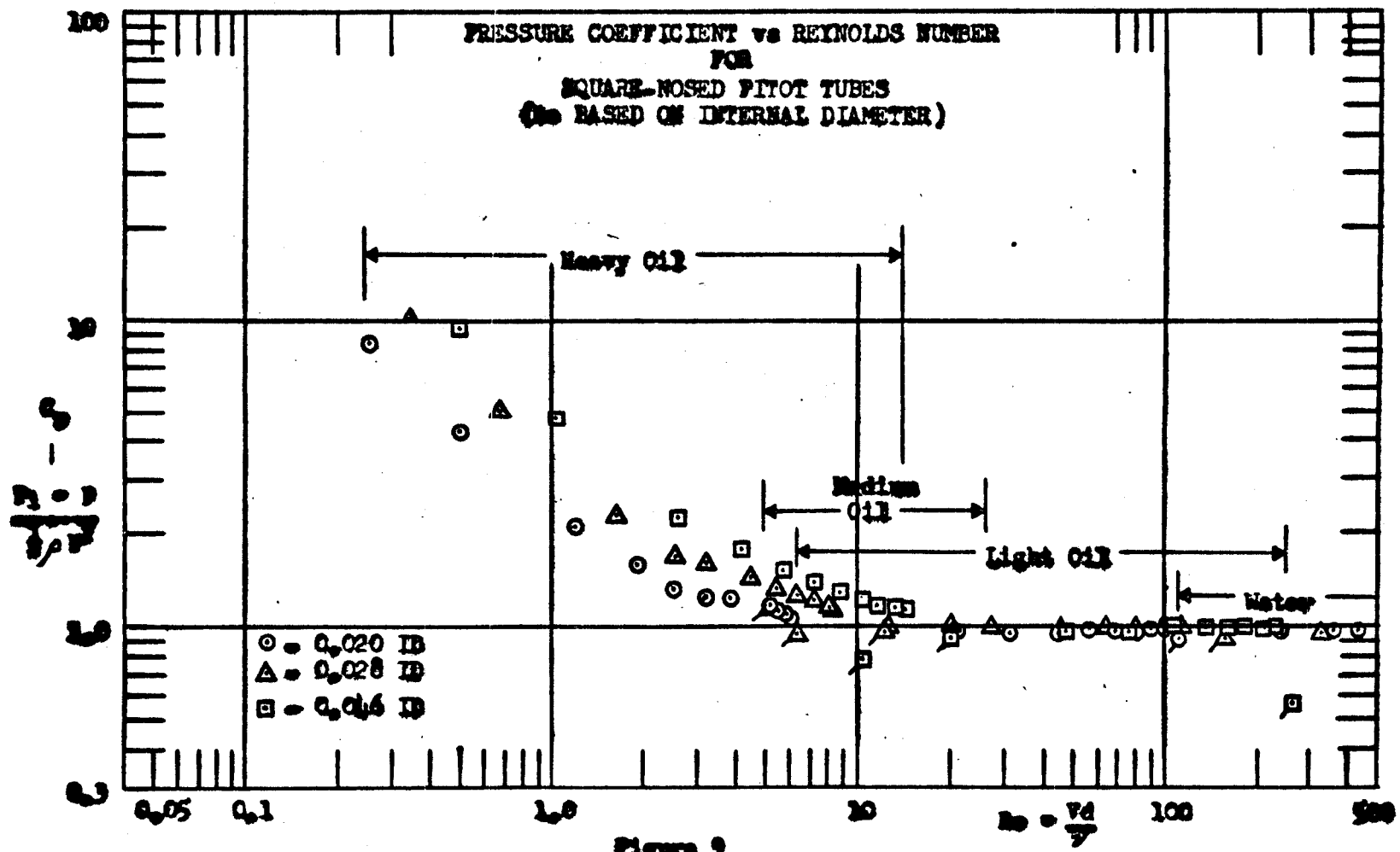
PRESSURE COEFFICIENT vs REYNOLDS NUMBER
FOR
SQUARE-NOSED PITOT TUBES
(Re BASED ON INTERNAL DIAMETER)
Heavy Oil
Medium Oil
Light Oil
Water
⊙ = 0.020 ID
△ = 0.028 ID
□ = 0.046 ID
100
10
1.0
0.3
0.05
0.1
1.0
10
100
500

Figure 9

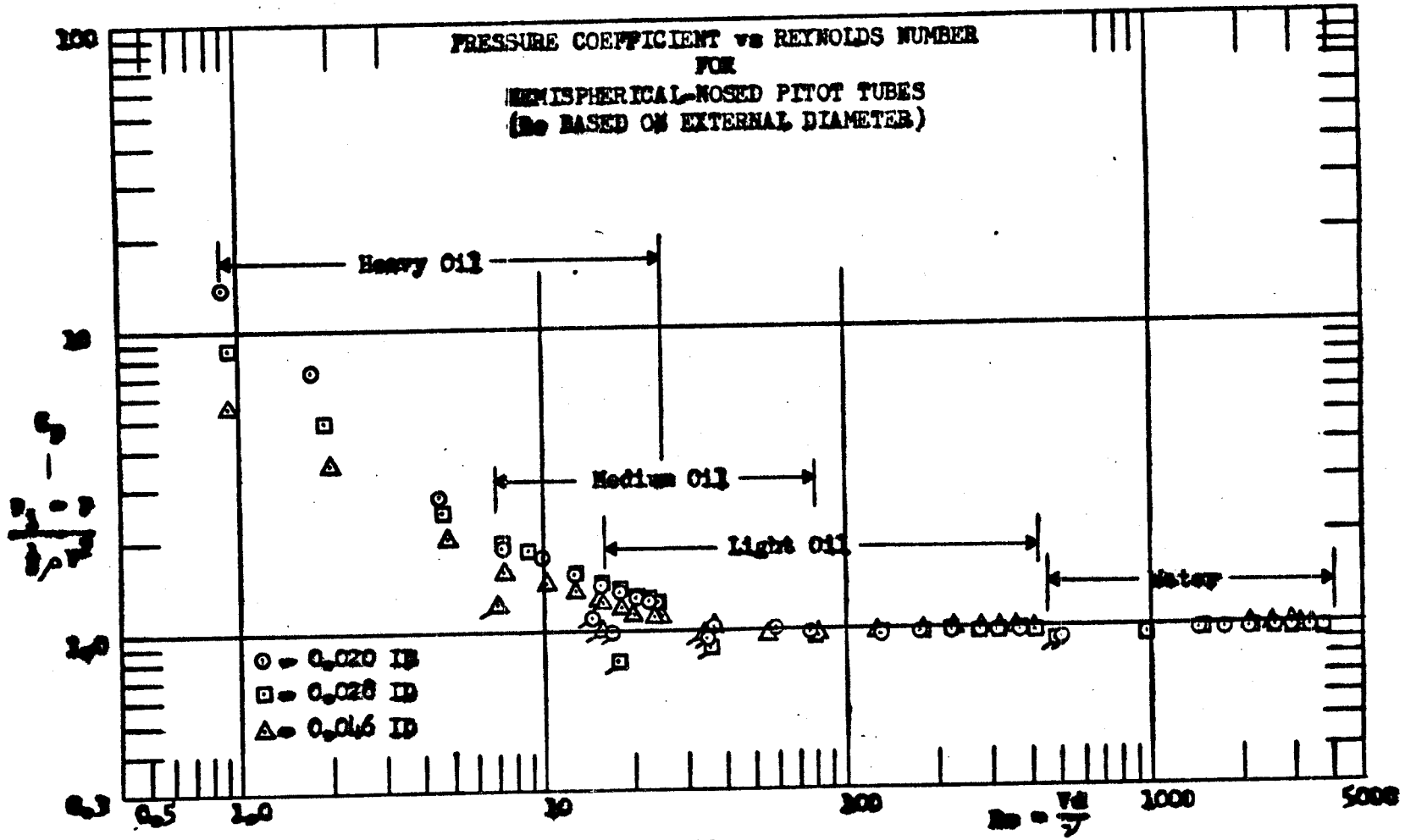
PRESSURE COEFFICIENT vs REYNOLDS NUMBER
FOR
HEMISPHERICAL-NOSED PITOT TUBES
(Re BASED ON EXTERNAL DIAMETER)
Heavy Oil
Medium Oil
Light Oil
Water
○ = 0.020 ID
□ = 0.028 ID
△ = 0.046 ID
100
10
1.0
0.3
0.5
1.0
10
100
1000
5000

Figure 10

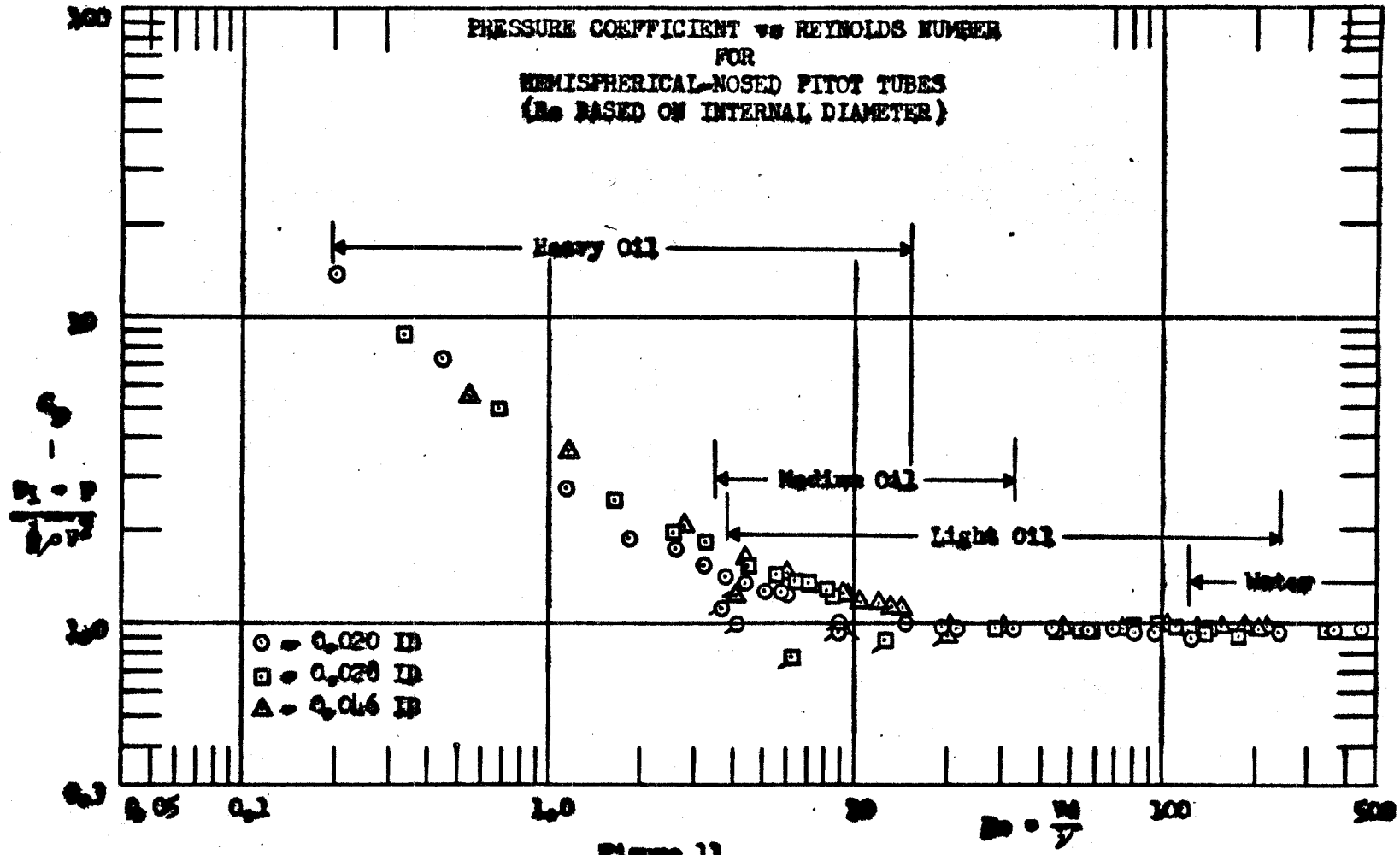
PRESSURE COEFFICIENT vs REYNOLDS NUMBER
FOR
HEMISPHERICAL-NOSED PITOT TUBES
(Re BASED ON INTERNAL DIAMETER)
Heavy Oil
Medium Oil
Light Oil
Water
○ = 0.020 ID
□ = 0.028 ID
△ = 0.046 ID
100
10
1.0
0.3
0.05
0.1
1.0
10
100
500

Figure 11

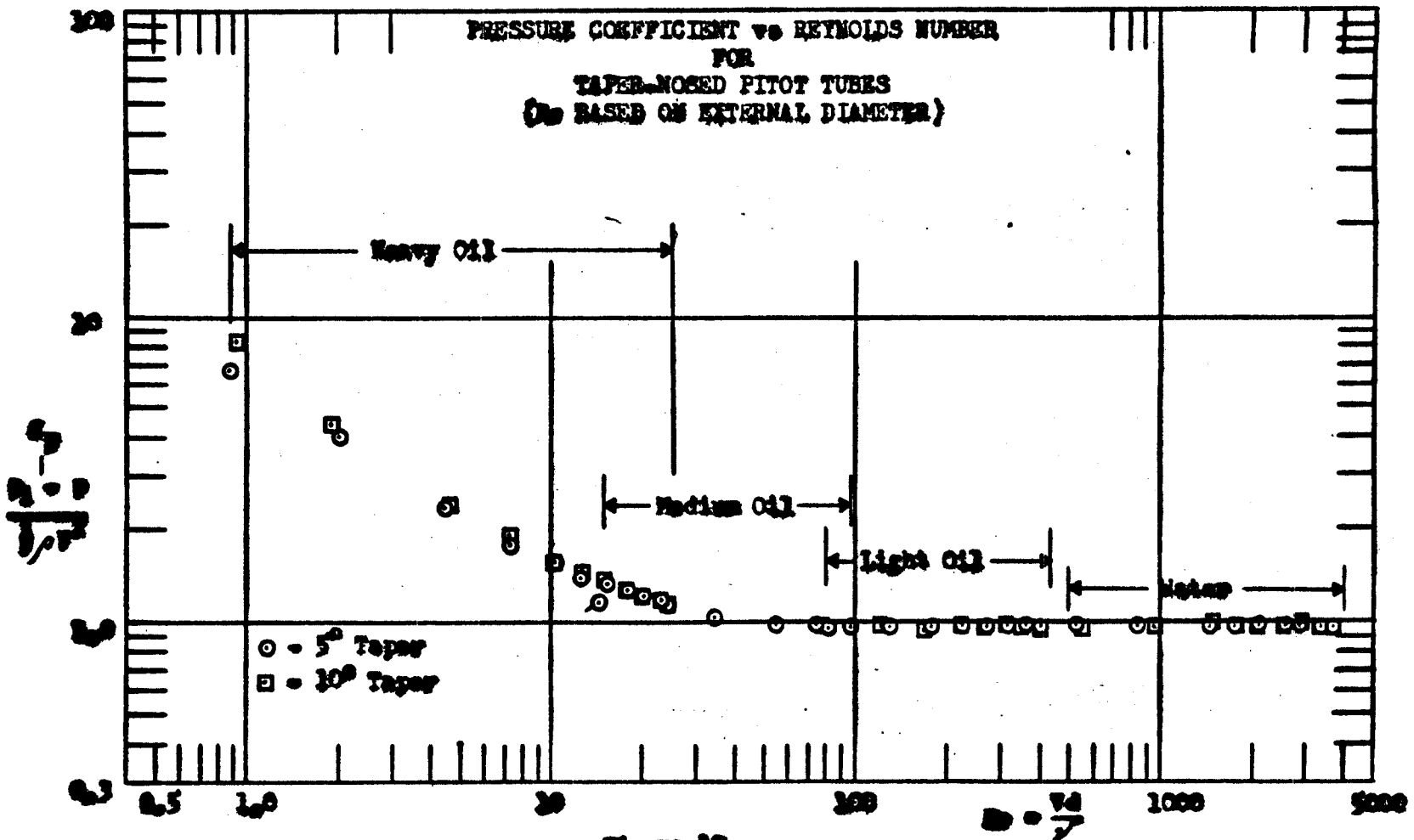
PRESSURE COEFFICIENT vs REYNOLDS NUMBER
FOR
TAPER-NOSED PITOT TUBES
(Re BASED ON EXTERNAL DIAMETER)
Heavy Oil
Medium Oil
Light Oil
○ = 5° Taper
□ = 10° Taper
0.5
1.0
20
100
1000

Figure 12

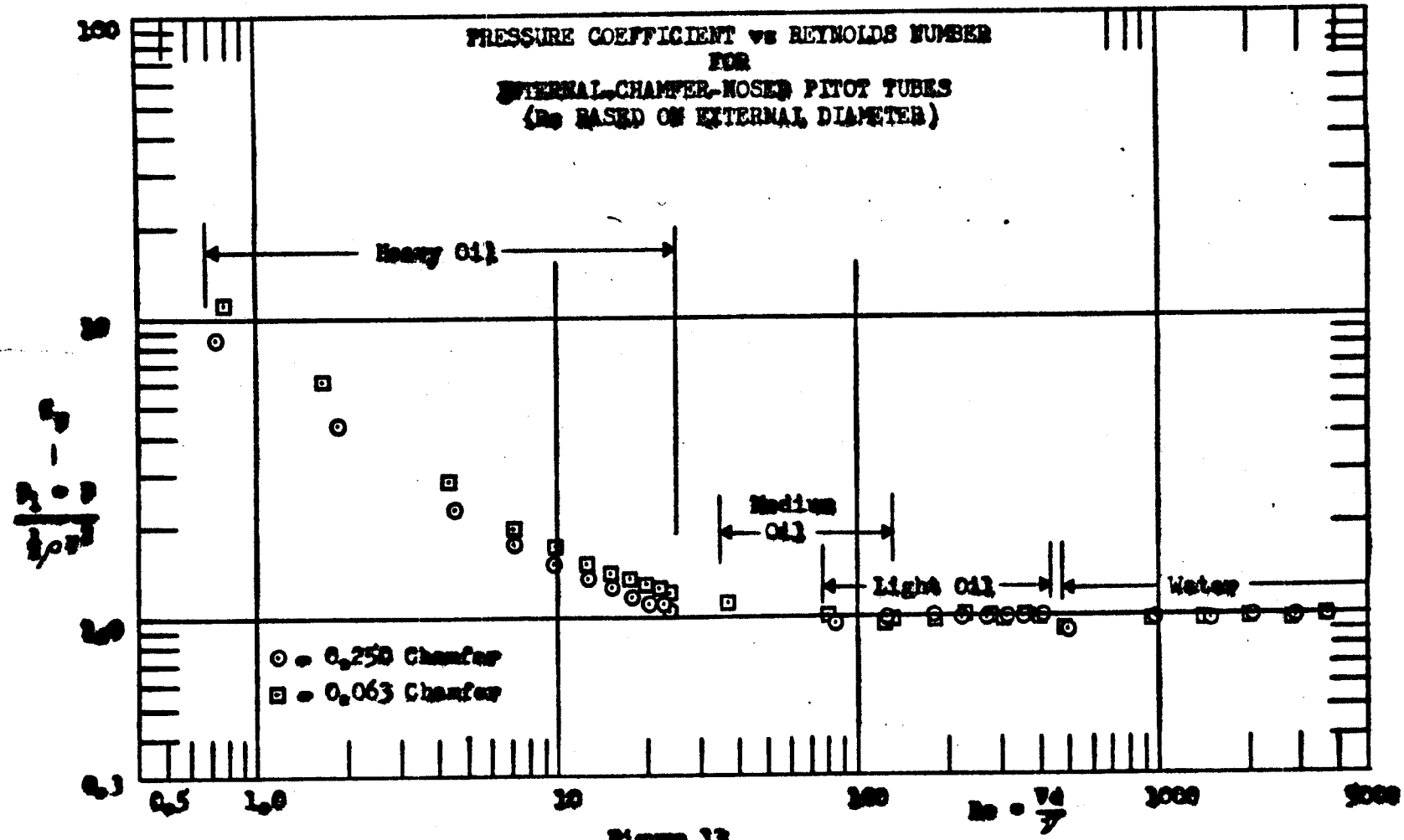
PRESSURE COEFFICIENT vs REYNOLDS NUMBER
FOR
EXTERNAL-CHAMFER-NOSED PITOT TUBES
(Re BASED ON EXTERNAL DIAMETER)
Heavy Oil
Medium Oil
Light Oil
Water
○ = 0.250 Chamfer
□ = 0.063 Chamfer
100
10
1.0
0.1
0.5
1.0
10
100
1000
Re = Vd/ν

Figure 13

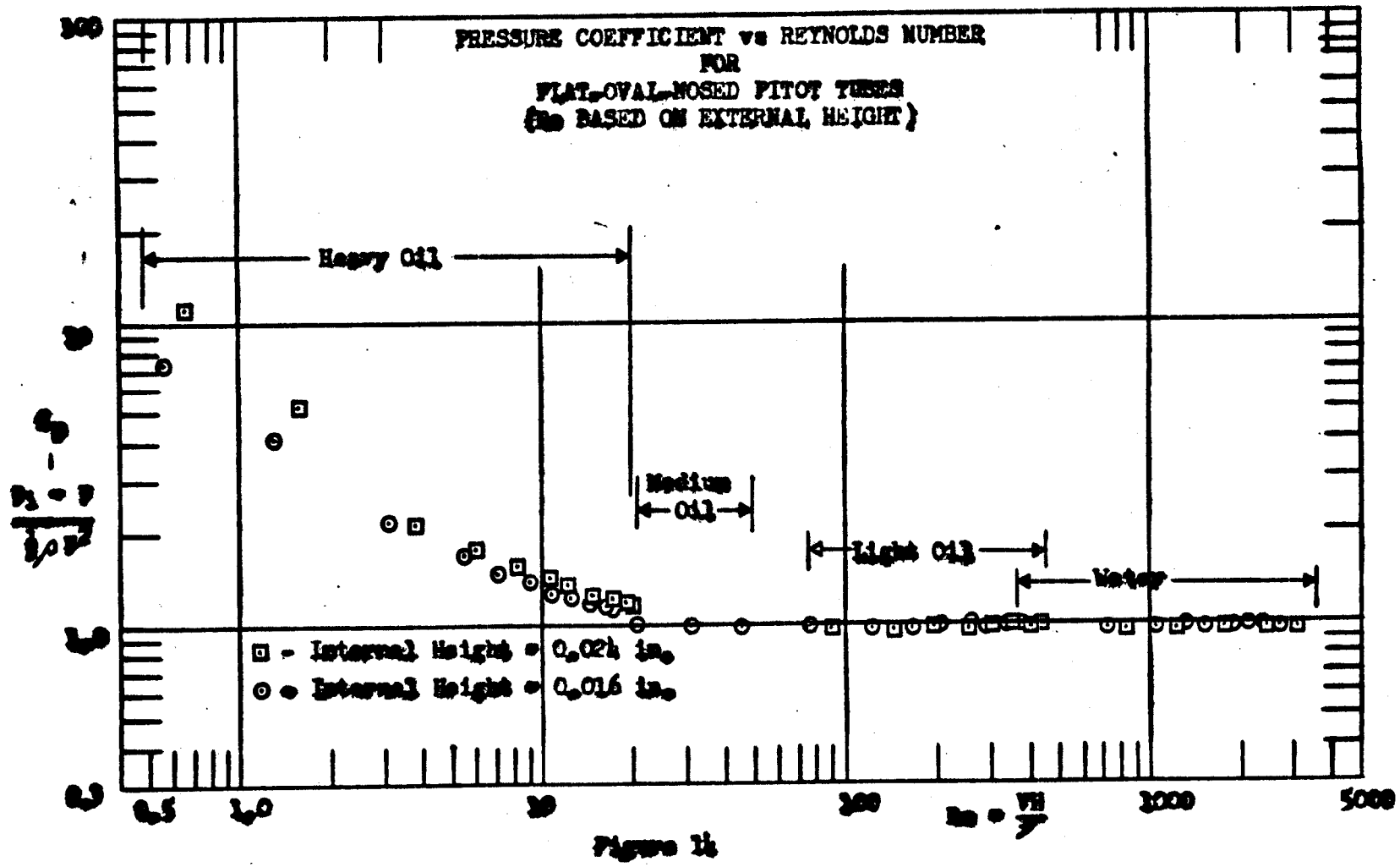
PRESSURE COEFFICIENT vs REYNOLDS NUMBER
FOR
FLAT-OVAL-NOSED PITOT TUBES
(Re BASED ON EXTERNAL HEIGHT)
Heavy Oil
Medium Oil
Light Oil
Water
□ - Internal Height = 0.024 in.
⊙ - Internal Height = 0.016 in.
0.5
1.0
10
100
1000
5000

Figure 14

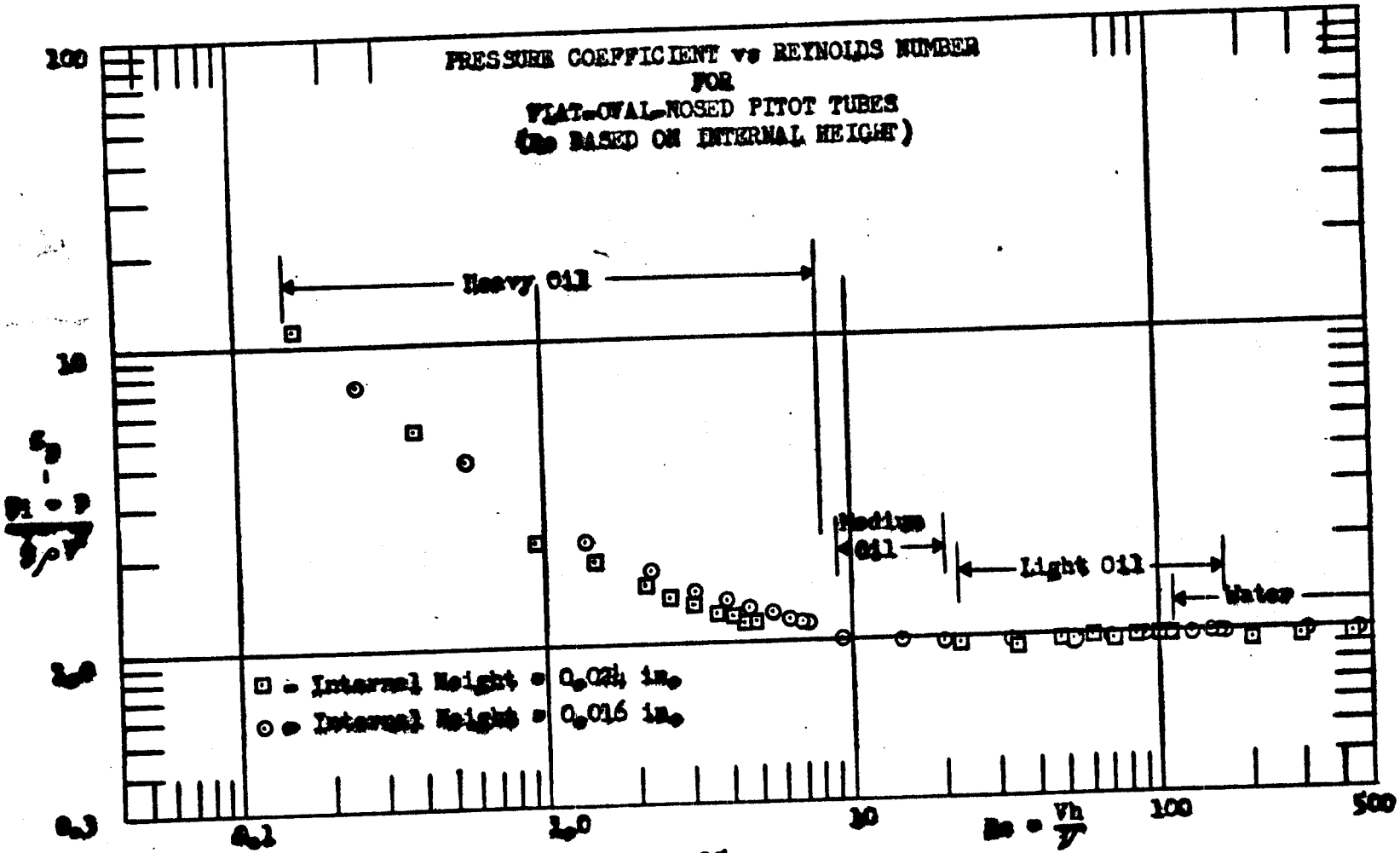
PRESSURE COEFFICIENT vs REYNOLDS NUMBER
FOR
FLAT-OVAL-NOSED PITOT TUBES
(Re BASED ON INTERNAL HEIGHT)
Heavy Oil
Medium Oil
Light Oil
Water
□ - Internal Height = 0.024 in.
⊙ - Internal Height = 0.016 in.
100
10
2.0
0.3
0.1
1.0
10
100
500

Figure 15

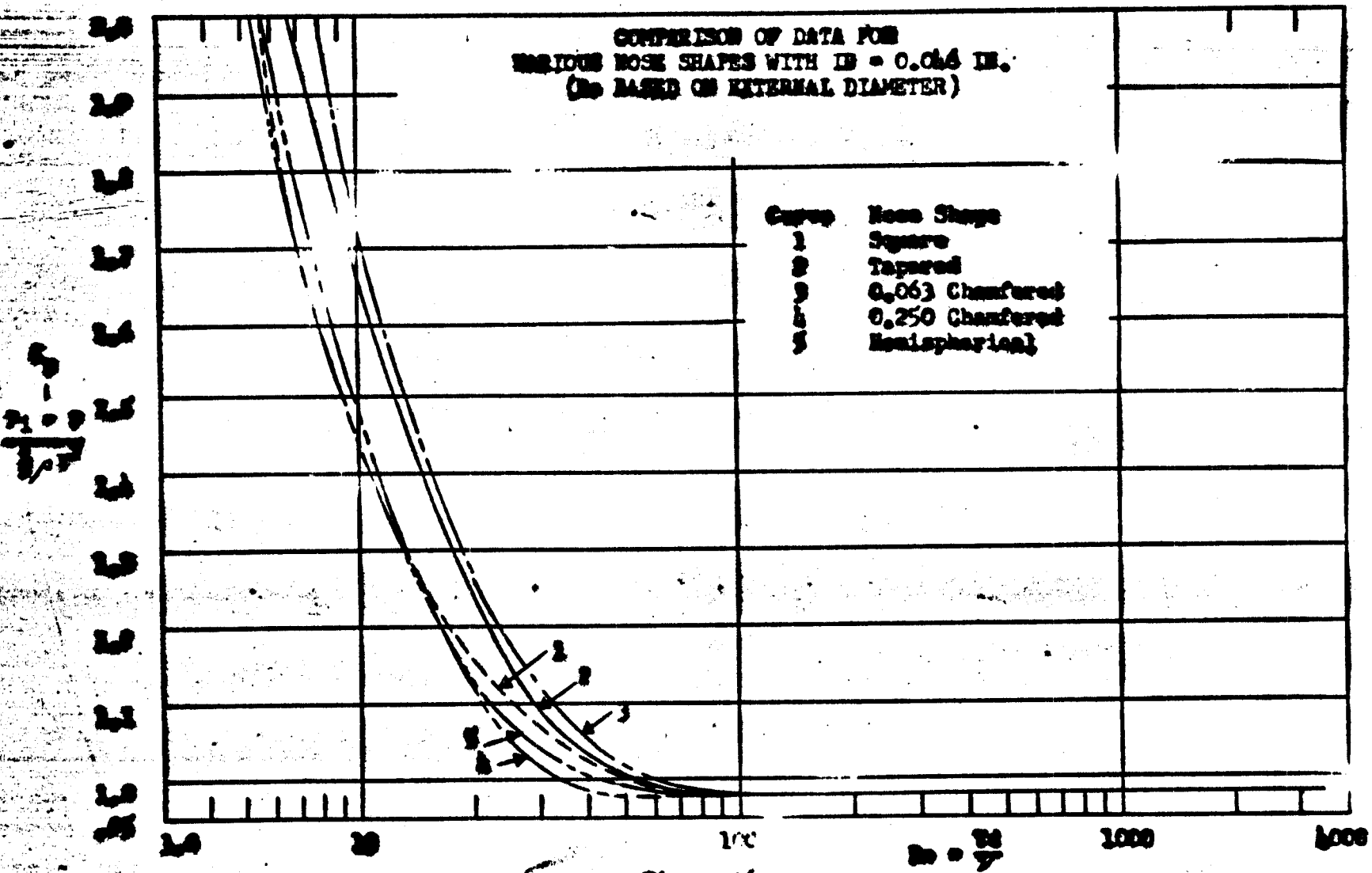
COMPARISON OF DATA FOR
VARIOUS NOSE SHAPES WITH ID = 0.046 IN.
(Do BASED ON EXTERNAL DIAMETER)
Curve Nose Shape
1 Square
2 Tapered
3 0.063 Chamfered
4 0.250 Chamfered
5 Hemispherical
1000

Figure 16

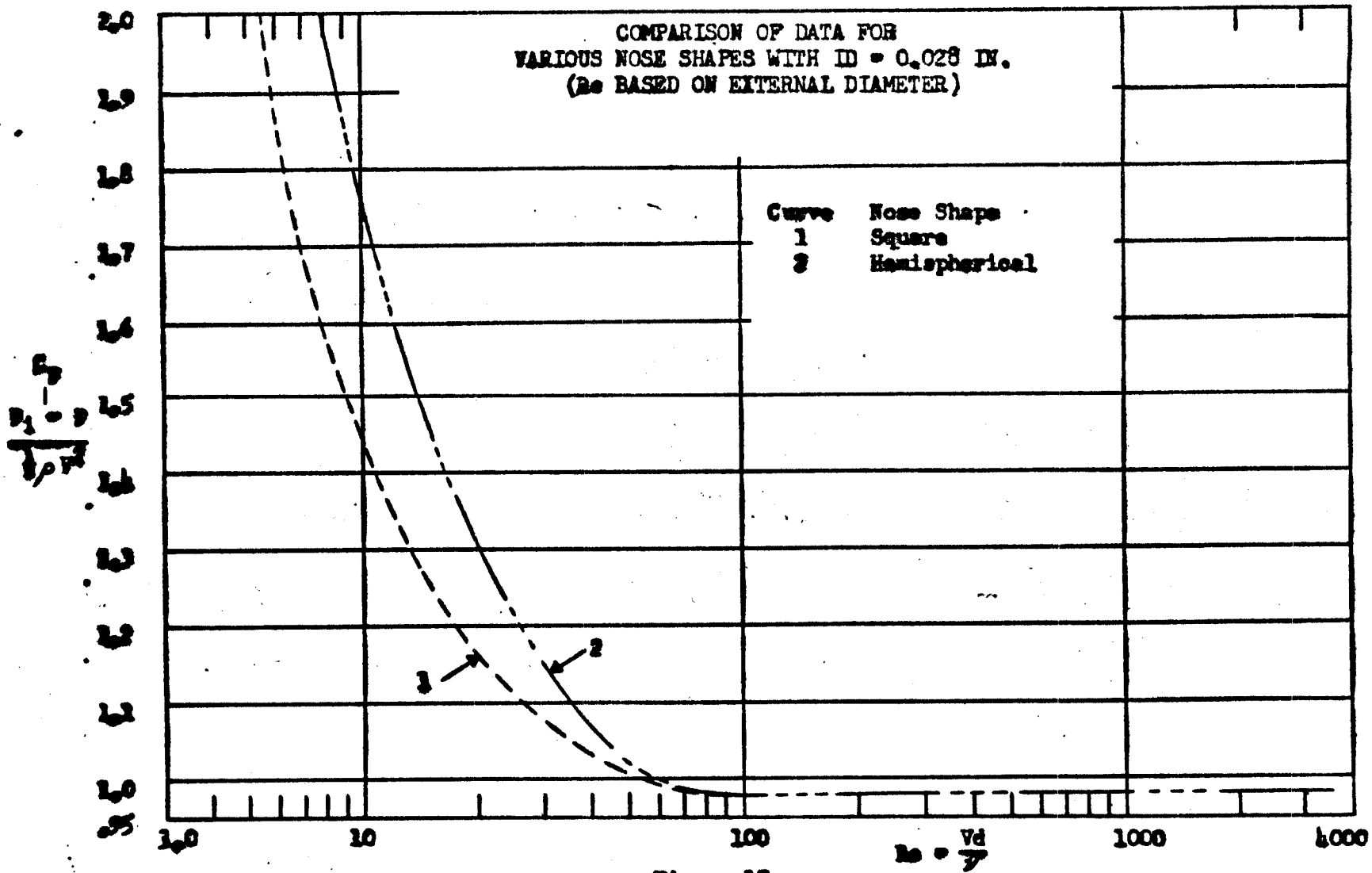
COMPARISON OF DATA FOR
VARIOUS NOSE SHAPES WITH ID = 0.028 IN.
(Re BASED ON EXTERNAL DIAMETER)
Curve Nose Shape
1 Square
2 Hemispherical
1
2
2.0
1.9
1.8
1.7
1.6
1.5
1.4
1.3
1.2
1.1
1.0
.95
1.0
10
100
1000
4000
Re = Vd/ν

Figure 17

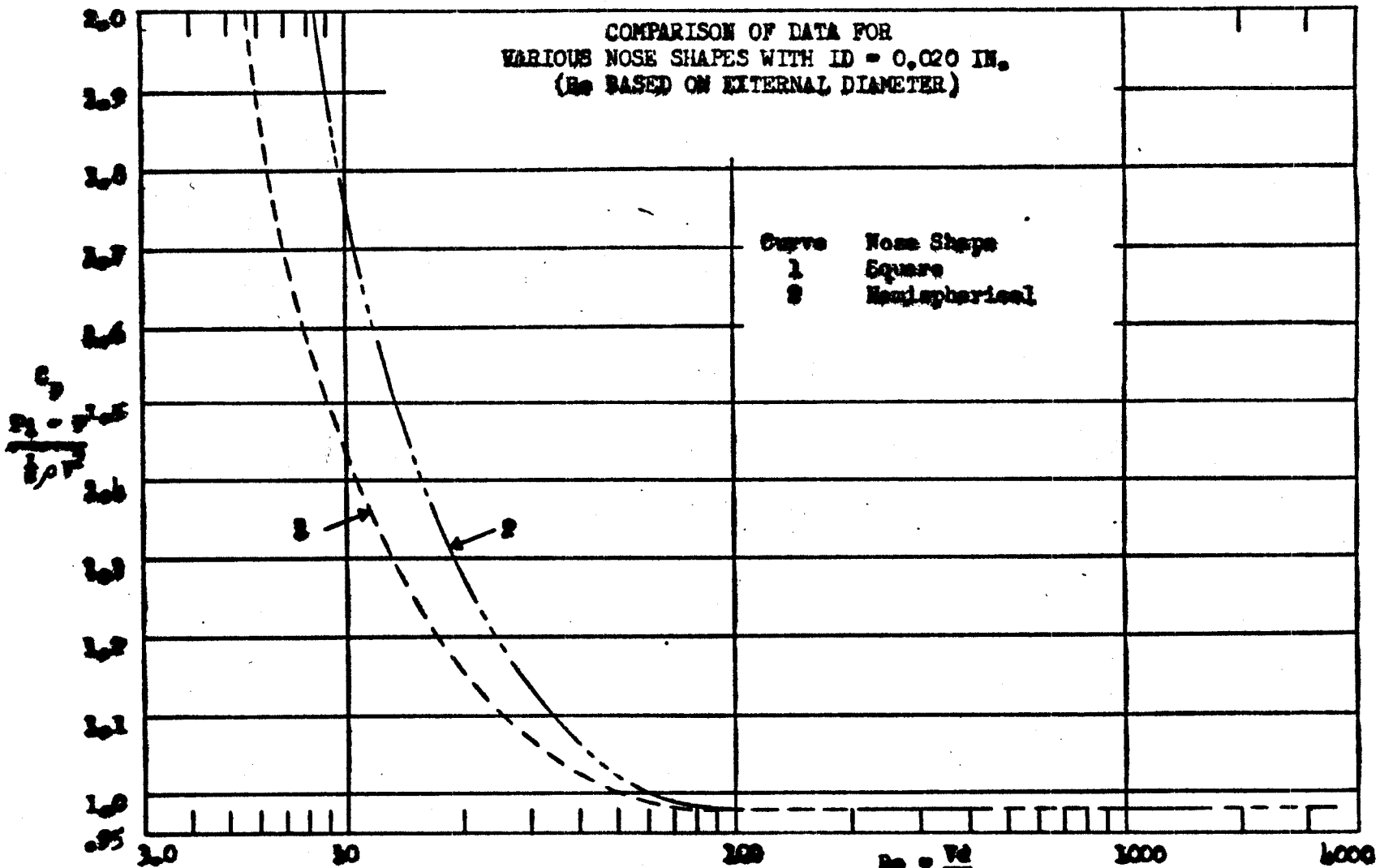
COMPARISON OF DATA FOR
VARIOUS NOSE SHAPES WITH ID = 0.020 IN.
(Re BASED ON EXTERNAL DIAMETER)
Curve Nose Shape
1 Square
2 Hemispherical
1
2
3.0
10
100
1000
4000
Re = Vd/ν

Figure 18

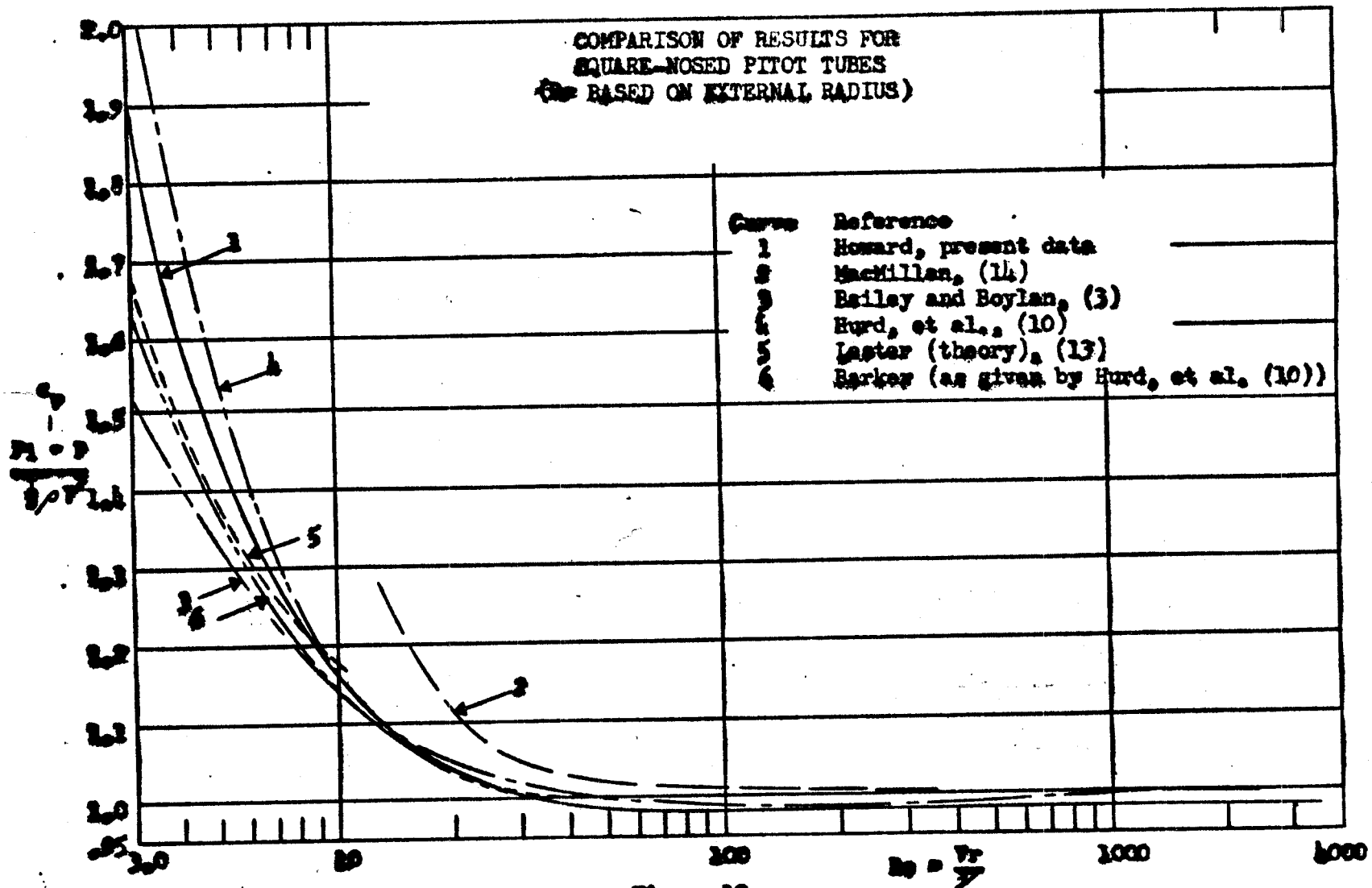
COMPARISON OF RESULTS FOR
SQUARE-NOSED PITOT TUBES
(Re BASED ON EXTERNAL RADIUS)
Curve Reference
1 Howard, present data
2 MacMillan, (14)
3 Bailey and Boylan, (3)
4 Hurd, et al., (10)
5 Lester (theory), (13)
6 Barker (as given by Hurd, et al. (10))
2.0
1.9
1.8
1.7
1.6
1.5
1.4
1.3
1.2
1.1
1.0
.95
20
100
1000
4000

Figure 19

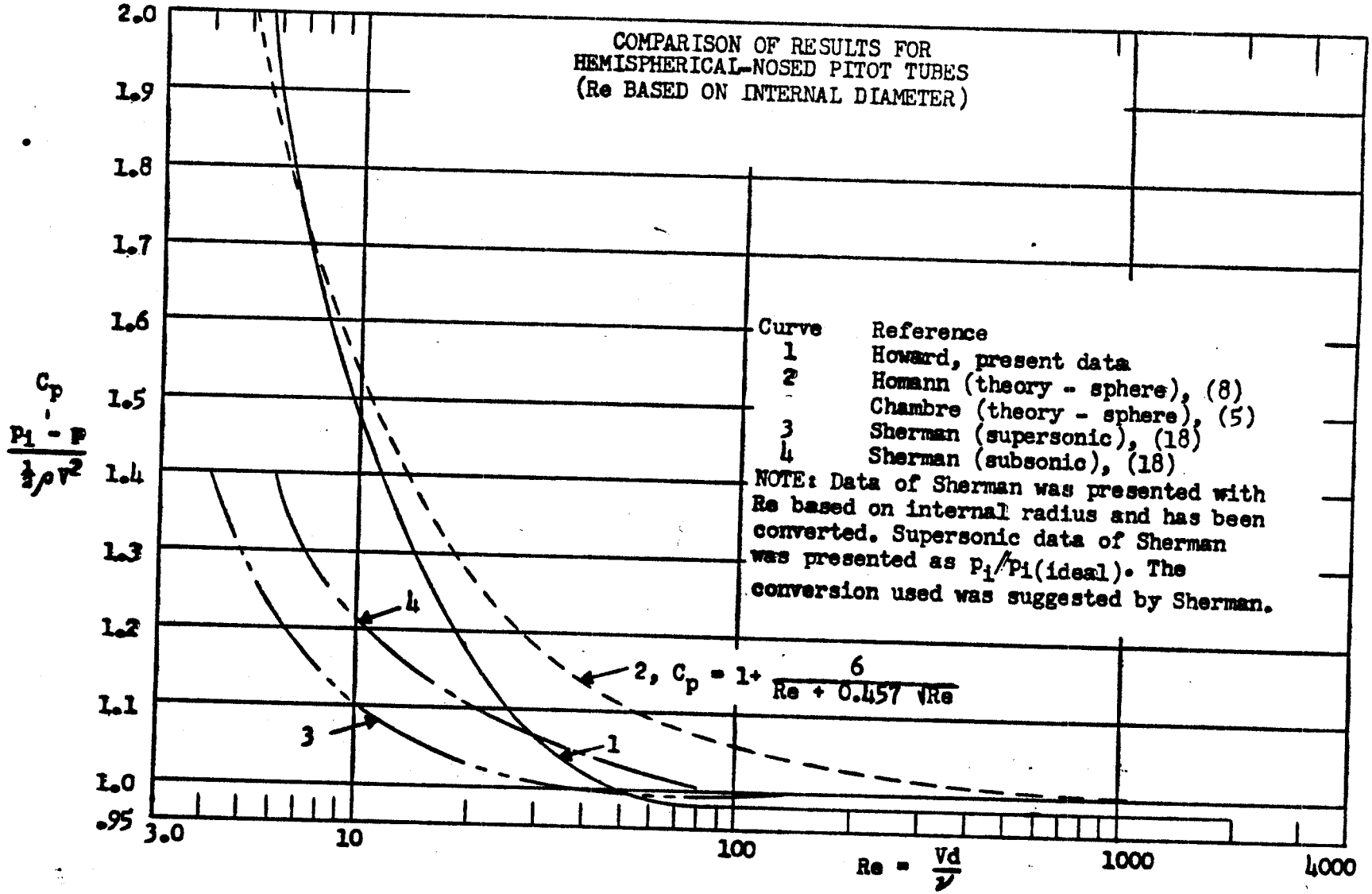
COMPARISON OF RESULTS FOR
HEMISPHERICAL-NOSED PITOT TUBES
(Re BASED ON INTERNAL DIAMETER)
Curve Reference
1 Howard, present data
2 Homann (theory - sphere), (8)
Chambre (theory - sphere), (5)
3 Sherman (supersonic), (18)
4 Sherman (subsonic), (18)
NOTE: Data of Sherman was presented with Re based on internal radius and has been converted. Supersonic data of Sherman was presented as $p_1/p_{i(ideal)}$. The conversion used was suggested by Sherman.
2, $C_p = 1 + \frac{6}{Re + 0.457\sqrt{Re}}$
$\frac{C_p}{\frac{p_1 - p}{\frac{1}{2}\rho V^2}}$
2.0
1.9
1.8
1.7
1.6
1.5
1.4
1.3
1.2
1.1
1.0
.95
3.0
10
100
1000
4000
$Re = \frac{Vd}{\nu}$

Figure 20

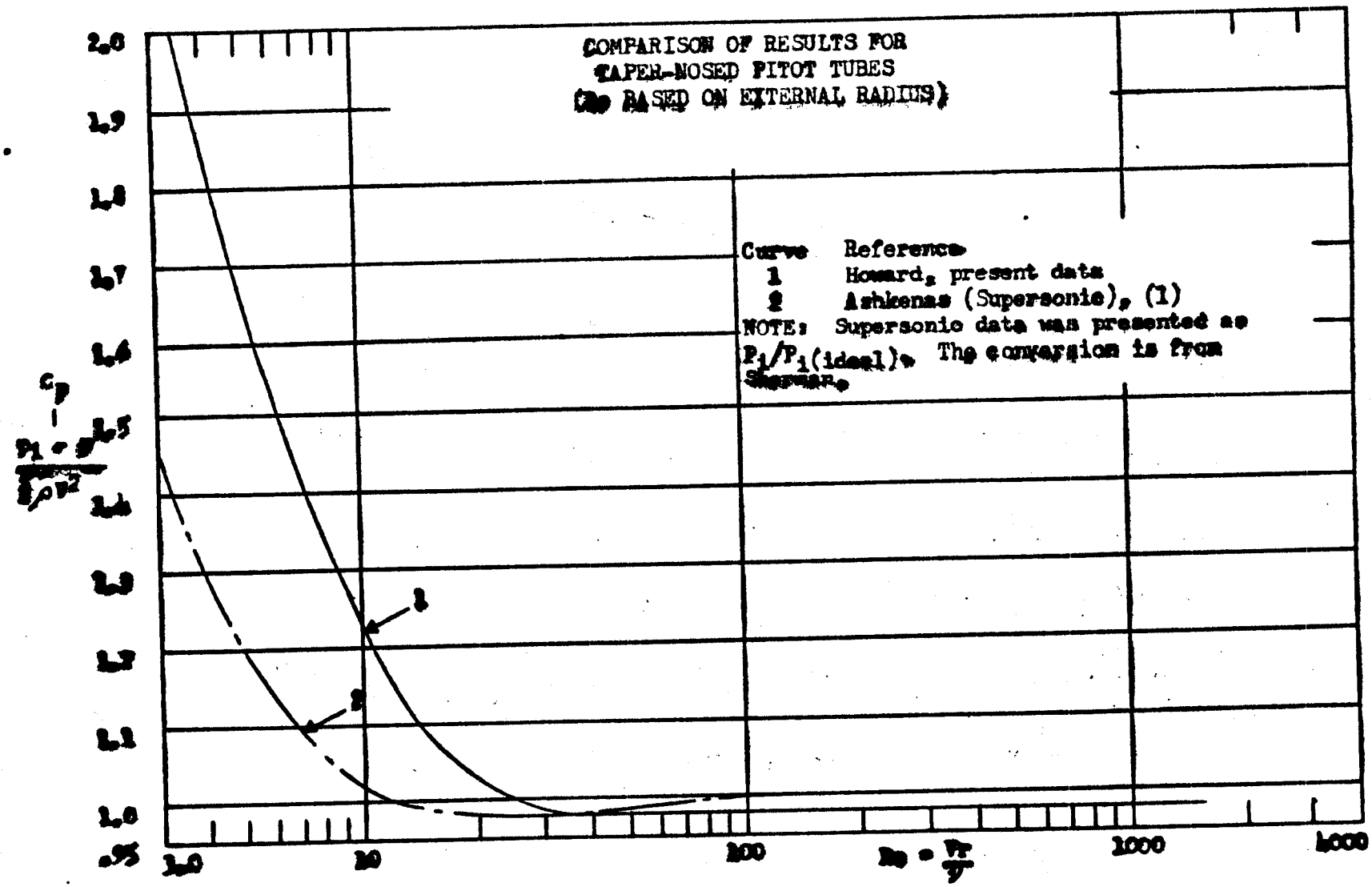
COMPARISON OF RESULTS FOR
TAPER-NOSED PITOT TUBES
(Re BASED ON EXTERNAL RADIUS)
Curve Reference
1 Howard, present data
2 Ashkenas (Supersonic), (1)
NOTE: Supersonic data was presented as
$P_1/P_{1(ideal)}$. The conversion is from
Shapiro.
2.0
1.9
1.8
1.7
1.6
1.5
1.4
1.3
1.2
1.1
1.0
.95
10
100
1000
1
2

Figure 21

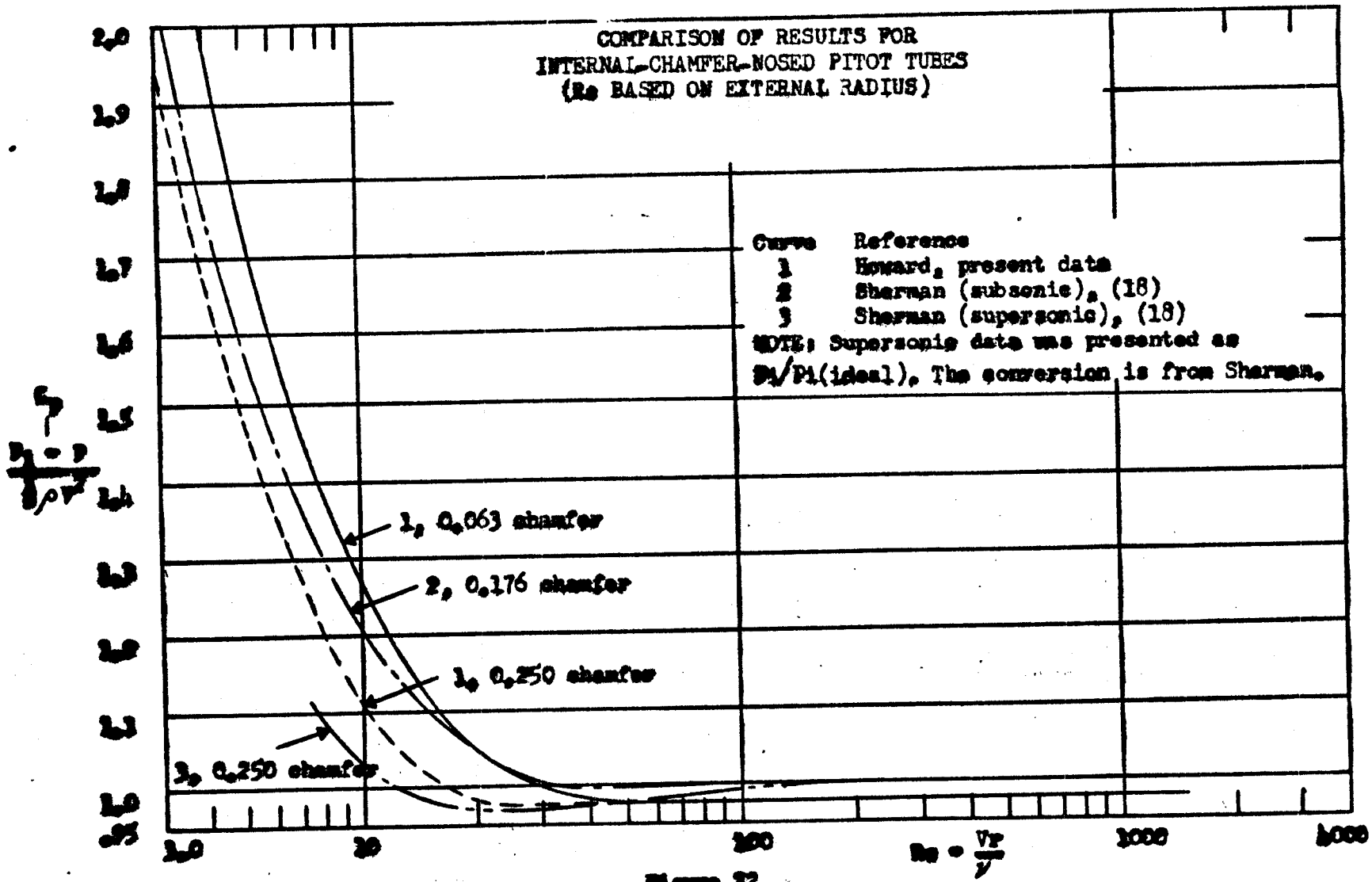
COMPARISON OF RESULTS FOR
INTERNAL-CHAMFER-NOSED PITOT TUBES
(Re BASED ON EXTERNAL RADIUS)
Curve Reference
1 Howard, present data
2 Sherman (subsonic), (18)
3 Sherman (supersonic), (18)
NOTE: Supersonic data was presented as
P1/P1(ideal). The conversion is from Sherman.
1, 0.063 chamfer
2, 0.176 chamfer
4, 0.250 chamfer
3, 0.250 chamfer
2.0
2.9
2.8
2.7
2.6
2.5
2.4
2.3
2.2
2.1
2.0
1.95
10
100
1000
10000
Re = Vr/ν

Figure 22

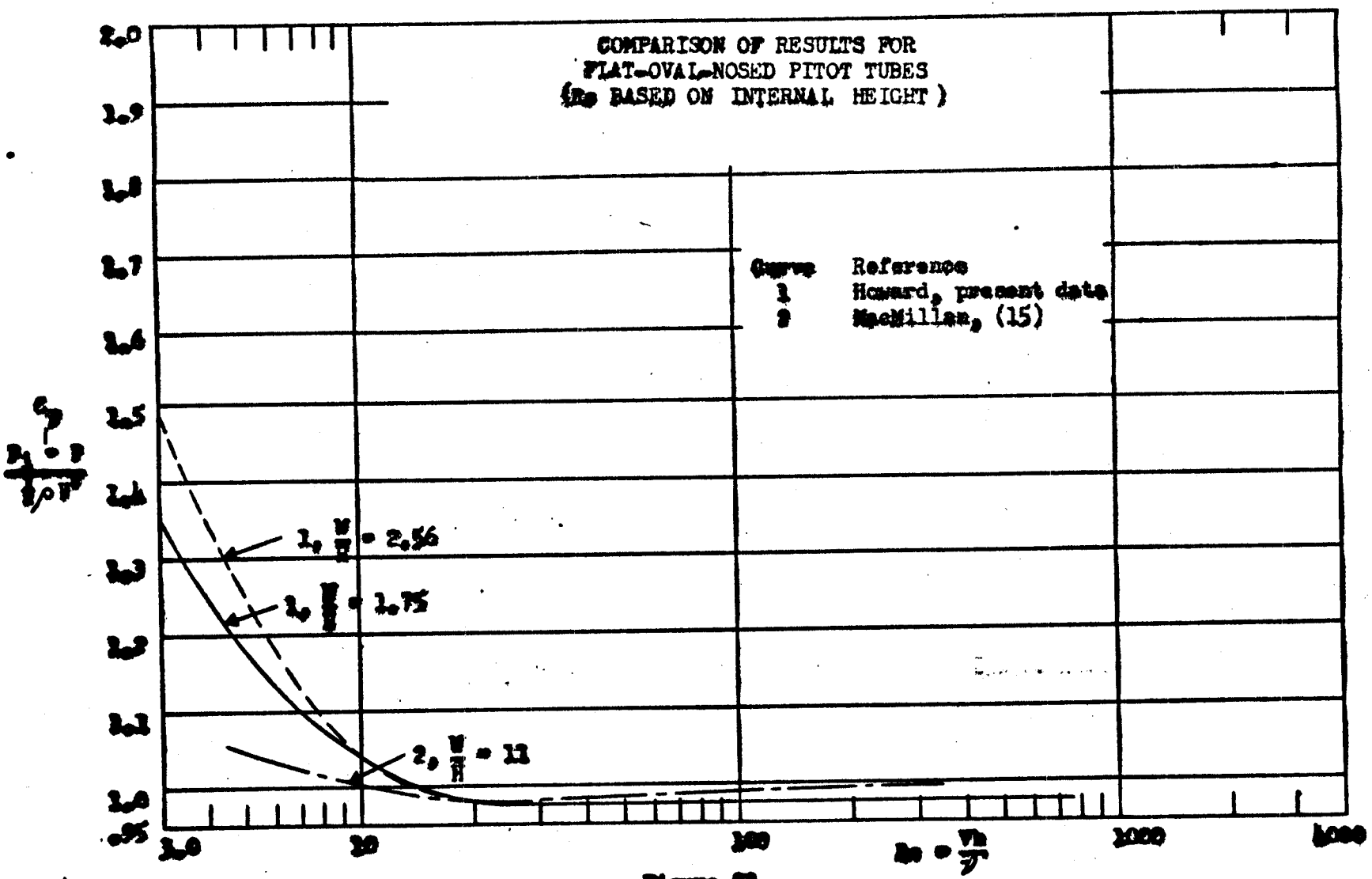
COMPARISON OF RESULTS FOR
FLAT-OVAL-NOSED PITOT TUBES
(Re BASED ON INTERNAL HEIGHT)
Curve
1
2
Reference
Howard, present data
MacMillan, (15)
2.0
1.9
1.8
1.7
1.6
1.5
1.4
1.3
1.2
1.1
1.0
.95
3.0
10
100
1000
$\frac{C_p}{\frac{p_1 - p}{\frac{1}{2}\rho V^2}}$
$Re = \frac{Vh}{\nu}$
$2, \frac{W}{H} = 2.56$
$2, \frac{W}{H} = 1.75$
$2, \frac{W}{H} = 11$

Figure 23

APPENDIX C

DATA SAMPLES

TABLE II: SAMPLE DATA

Hemispherical Nose

OD: 0.078 in. ID: 0.046 in. Fluid: Heavy Oil $\nu = 356 \times 10^{-5}$ ft.^{2}/sec.

Variac	Time	Time_{ave}	Rev	rpm	V - fps	β	β_{ave}	$\alpha = \beta_{ave} - 90^\circ$
0	0	0	0	0	0	98°23'53" 98°23'53.5" 98°23'52.5"	98°23'53"	8°23'53"
9.6	0.390 0.390 0.390	0.390	10	25.65	13.41	95°54'10.8" 54'6.1" 54'6.2"	95°54'7.7"	5°54'7.7"
9.0	0.416 0.417 0.412	0.415	10	24.10	12.61	59'16.3" 59'12.3" 59'17.9"	95°59'15.5"	5°59'15.5"
8.0	0.467 0.463 0.468	0.466	10	21.45	11.23	96°3'6.0" 3'8.6" 3'4.9"	96°3'6.5"	6°3'6.5"
7.0	0.528 0.528 0.530	0.529	10	18.92	9.90	13'41.0" 13'41.3" 13'39.2"	96°13'40.5"	6°13'40.5"
6.0	0.613 0.610 0.612	0.612	10	16.33	8.55	25'3.0" 24'59.0" 24'58.1"	96°25'0.0"	6°25'0.0"
5.0	0.743 0.750 0.743	0.745	10	13.42	7.02	36'54.8" 36'55.1" 36'54.2"	96°36'54.7"	6°36'54.7"

TABLE II: SAMPLE DATA (cont.)

Variac	Time	$Time_{ave}$	Rev.	rpm	V - fps	β	β_{ave}	$\alpha = \beta_{ave} - 90^\circ$
4.0	0.930 0.932 0.930	0.931	10	10.74	5.62	52'28.8" 52'28.2" 52'29.3"	96°52'28.8"	6°52'28.8"
3.0	1.273 1.273 1.273	1.273	10	7.85	4.11	97°13'24.6" 13'21.6" 13'23.0"	97°13'23.1"	7°13'23.1"
2.0	2.010 2.003 2.010	2.008	10	4.98	2.61	37'24.5" 37'28.6" 37'27.2"	97°37'26.8"	7°37'26.8"
1.0	4.760 4.762 4.761	4.761	10	2.10	1.099	98°3'12.0" 3'13.0" 3'12.5"	98°3'12.5"	8°3'12.5"
0.6	5.048 5.032 5.040	5.040	5	0.993	0.520	14'12.8" 14'12.0" 14'9.3"	98°14'11.4"	8°14'11.4"

SAMPLE CALCULATIONS

0.020 ID hemispherical nose in heavy oil

$V = 0.520$ fps

$V^2 = 0.271$ ft^2/sec^2

$\alpha = 8°14'11.4'' = 8.236°$

$d = 0.078$ in.

$\beta = 8°23'58'' = 8.399°$

$\nu = 356 \times 10^{-5}$ ft^2/sec

$c = 95.228 \tan \beta$

$c = 95.228 (0.1475)$

$c = 14.040$ in. $= 1.170$ ft

$h = c - 95.228 \tan \alpha$

$h = 1.170 - \frac{95.228}{12} (0.1449)$

$h = 1.170 - 1.149$

$h = 0.021$ ft

$$C_p = 1 + \frac{2gh}{V^2}$$

$$C_p = 1 + \frac{2(32.2)0.021}{0.271}$$

$$C_p = 1 + 4.490$$

$$C_p = 5.490$$

$$Re = \frac{Vd}{12\nu}$$

$$Re = \frac{0.520(0.078)}{12(356 \times 10^{-5})}$$

$$Re = 0.950$$

BIBLIOGRAPHY

1. Ashkenas, H. I., "Pitot Tube Corrections in Low Density Flows," Jet Propulsion Laboratory, Pasadena California, Space Programs Summary No. 37 - 15, Vol. IV, June 30, 1962, pp. 123 - 124.

2. ASTM Standards, 1961, part 7, "Petroleum Products and Lubricants," (American Society for Testing and Materials).

3. Bailey, A. B., Boylan, D. E., "Some Experiments on Impact Pressure Probes in a Low-Density Hypervelocity Flow," von Karman Gas Dynamics Facility, ARO, Inc., Report AEDC-TN-61-161, Dec., 1961.

4. Barker, M., "On the Use of Very Small Pitot-Tubes for Measuring Wind Velocity," Proceedings of the Royal Society, London, ser. A, Vol. 101, 1922, pp. 435-445.

5. Brenkert, Karl, Jr., Elementary Theoretical Fluid Mechanics (John Wiley and Sons, Inc., New York, 1960), pp. 53-56

6. Durand, W. F., Aerodynamic Theory (Dover Publications, Inc., New York, 1963), Vol. III, pp. 69-75.

7. Folsom, R. G., "Review of the Pitot Tube," The University of Michigan Industry Program of the College of Engineering, Ann Arbor, Michigan, Report IP-142, 1955.

8. Homann, F., "The Effect of High Viscosity on the Flow Around a Cylinder and Around a Sphere," NACA TM 1334, 1952

9. Humphreys, Milton D., "Effects of Compressibility and Large Angles of Yaw on Pressure Indicated by a Total-Pressure Tube," Langley Memorial Aeronautical Laboratory, Langley Field, Va., NACA Report L-77.

10. Hurd, C. W., Chesky, K. P., "Experimental Investigation of the Effect of Viscous Forces upon Pitot Tube Readings," Massachusetts Institute of Technology, Master's Thesis, 1951.

11. Hurd, C. W., Chesky, K. P. and Shapiro, A. A., "Influence of Viscous Effects on Impact Tubes," Journal of Applied Mechanics, Vol. 20, No. 2, 1953.

12. Kellam, John M., Jr., "Experimental Investigation of Pressures on Impact Probes and Beveled Cylindrical Probes in a Low Density, Hypersonic Airstream," Aerodynamic Laboratory, Department of Aeronautical Engineering, The Ohio State University, Tech. Memo No. 18, Sept., 1959.

13. Lester, W. G. S., "The Flow Past a Pitot Tube at Low Reynolds Numbers," Department of Engineering Science, University of Oxford (Aeronautical Research Council, Fluid Motion Sub-Committee), Report A.R.C. 22,070, F.M. 2983, 1960.

14. MacMillan, F. A., "Viscous Effects on Pitot Tubes at Low Speeds," Engineering Laboratory, Cambridge (Aeronautical Research Council, Fluid Motion Sub-Committee), Report F.M. 2081, 1954.

15. MacMillan, F. A., "Viscous Effects on Flattened Pitot Tubes at Low Speeds," Aeronautical Research Council, Fluid Motion Sub-Committee, Report 17, 106, F.M. 2081a, Oct. 14, 1954.

16. Norton, Arthur E., Lubrication (McGraw-Hill Book Company, Inc., New York, 1942), pp. 46-61.

17. Salter, C., Warsap, J. H., and Goodman, Miss D. G., "A New Design of Pitot-Static Tube with a Discussion of Pitot-Static Tubes and their Calibration Factors," National Physical Laboratory, Aerodynamics Division, NPL Aero Rep. 1013, A.R.C. 23,760, F.M. 3186, May, 1962.

18. Sherman, F.S., "New Experiments on Impact-Pressure Interpretation in Supersonic and Subsonic Rarefied Air Streams," University of California, NACA Technical Note 2995, Sept., 1953.